Eur. Phys. J. B **25**, 373–389 (2002)
DOI: 10.1140/epjb/e20020042

THE EUROPEAN PHYSICAL JOURNAL B
EDP Sciences

Microscopic theory of non local pair correlations in metallic F/S/F trilayers

V. Apinyan and R. Mélin[a]

Centre de Recherches sur les Très Basses Températures (CRTBT)[b], CNRS BP 166X, 38042 Grenoble Cedex, France

Received 4 July 2001 and Received in final form 8 November 2001

Abstract. We consider a microscopic theory of F/S/F trilayers with metallic or insulating ferromagnets. The trilayer with metallic ferromagnets is controlled by the formation of non local pair correlations among the two ferromagnets which do not exist with insulating ferromagnets. The difference between the insulating and ferromagnetic models can be understood from lowest order diagrams. Metallic ferromagnets are controlled by non local pair correlations and the superconducting gap is larger if the ferromagnetic electrodes have a parallel spin orientation. Insulating ferromagnets are controlled by pair breaking and the superconducting gap is smaller if the ferromagnetic electrodes have a parallel spin orientation. The same behavior is found in the presence of disorder in the microscopic phase variables and also in the presence of a partial spin polarization of the ferromagnets. The different behaviors of the metallic and insulating trilayers may be probed in experiments.

PACS. 74.50.+r Proximity effects, weak links, tunneling phenomena, and Josephson effects – 74.80.Dm Superconducting layer structures: superlattices, heterojunctions, and multilayers

1 Introduction

Spin polarized quantum transport has focussed an important interest recently. One of the challenges in this field of research is to manipulate correlated pairs of electrons in solid state devices. Several possibilities have been proposed recently [1–6], some of which involve superconductivity and magnetism.

There is a rich physics occurring at a single F/S interface. For instance it is well established that the superconducting order parameter induced in a ferromagnetic metal can oscillate in space [7–10]. In S/F/S Josephson junctions these oscillations can induce a change of sign in the Josephson coupling [11]. This gives rise to the π-state that has been probed recently in two experiments [12,13]. Another effect taking place at F/S interfaces is the suppression of Andreev reflection by spin polarization [14]. This has been probed in recent transport experiments, either with highly transparent point contacts [15] or with intermediate interface transparencies [16]. Other systems such as F/S interfaces in diffusive heterostructures have been the subject of several experimental investigations [17–22]. These works have generated many theoretical discussions (see for instance Refs. [23–30]).

The specific features associated to transport in multiterminal systems have been discussed recently with various methods such as Landauer formalism [3], lowest order perturbation for low transparency interfaces [4] or non perturbative solutions for high transparency interfaces [6]. It was shown theoretically that the conductance associated to Andreev reflection is equal to the conductance associated to elastic cotunneling [4,6]. This could be probed in future experiments by measuring the conductance as a function of the relative spin orientation of the ferromagnetic electrodes.

It is also important to understand equilibrium properties in multiterminal hybrid systems. The proximity effect at F/S interfaces has been discussed in details recently [31,32]. It is well established theoretically that there exists oscillations of the critical temperature in F/S multilayers as the exchange field and thickness of the F layer are varied [33]. These oscillations of the critical temperature have been probed experimentally in several systems: Nb/Gd multilayers [34,35], Nb/CuMn multilayers [36], Nb/Gd/Nb trilayers [37] and Fe/Nb/Fe trilayers [38]. Usadel equations have been applied recently to discuss diffusive F/S/F trilayers [39]. F/S/F trilayers have also been discussed recently in connection with possible device applications such as a superconducting magnetoresistive memory elements [40] or a superconducting spin switch [41]. The physics of the F/S/F trilayer with

[a] e-mail: melin@polycnrs-gre.fr
[b] UPR 5001 du CNRS, Laboratoire conventionné avec l'Université Joseph Fourier

insulating ferromagnets is controlled by pair breaking [42–44]. Single electron states in the superconductor are coupled to an effective exchange field that cancels if the two ferromagnets have an antiparallel spin orientation. As a consequence the superconducting gap is smaller if the ferromagnets have a parallel spin orientation.

F/S/F trilayers with metallic ferromagnets have been investigated in a recent work [45] on the basis of effective Green's functions. It was found that the physics is not controlled by pair breaking, contrary to the F/S/F trilayer with insulating ferromagnets. It was found that with metallic ferromagnets the superconducting gap is larger if the ferromagnetic electrodes have a parallel spin orientation [45]. It was proposed that the qualitative physics of multiterminal devices can be characterized by linear superpositions of pair states [45]. We can therefore contrast two different situations:

(i) F/S/F trilayers with insulating ferromagnets are controlled by single electron states. The superconducting order parameter is smaller if the ferromagnetic electrodes have a parallel spin orientation.
(ii) F/S/F trilayers with metallic ferromagnets are controlled by non local pair correlations. The superconducting order parameter is smaller if the ferromagnetic electrodes have an antiparallel spin orientation.

The goal of our article is to discuss F/S/F trilayers with metallic and insulating ferromagnets, as well as a "mixed" trilayer with an insulating and a metallic ferromagnet. We use two different approaches, either analytical (with some approximations) or based on exact diagonalizations.

The article is organized as follows. The model is given in Section 2, as well as technical preliminaries. Half-metal ferromagnets are discussed in Section 3. This discussion is extended in Section 3.6 to describe an arbitrary exchange field. We present exact diagonalizations in Section 4. Final remarks are given in Section 5.

2 Preliminaries

2.1 The model

We consider throughout the article a superconductor in contact with several ferromagnetic electrodes. The superconductor is three dimensional but a one dimensional geometry will also be used in the numerical simulations. We describe the superconductor by a tight binding BCS model in which the electrons can hop between neighboring "sites" on a square lattice having a lattice parameter a_0. The BCS Hamiltonian takes the form

$$\mathcal{H}_{\rm BCS} = \sum_{\langle\alpha,\beta\rangle,\sigma} -t\left(c^+_{\alpha,\sigma}c_{\beta,\sigma} + c^+_{\beta,\sigma}c_{\alpha,\sigma}\right) + \sum_{\alpha}\left(\Delta_\alpha c^+_{\alpha,\uparrow}c^+_{\alpha,\downarrow} + \Delta^*_\alpha c_{\alpha,\downarrow}c_{\alpha,\uparrow}\right), \quad (1)$$

where the summation in the kinetic term is carried out over neighboring pairs of sites. Without loss of generality, we assume that the superconductor conduction band is half-filled with therefore $k_{\rm F}a_0 = \pi/2$. We note $\epsilon_{\rm F}$ the Fermi energy ($\epsilon_{\rm F} = t$ for a half-filled band) and we use also the notation D for the bandwidth. The physics does not depend on the details of the band structure. Rather than using a tight-binding model we can also use the free electron dispersion relation $\epsilon(k) = \frac{\hbar^2k^2}{2m}$, with $\epsilon_{\rm F} = \frac{\hbar^2k_{\rm F}^2}{2m}$ the Fermi energy. This dispersion relation is truncated by a high energy cut-off $\epsilon(k_{\rm max}) = 2D = 2\epsilon_{\rm F}$.

The ferromagnetic electrodes are described by the Stoner model

$$\mathcal{H}_{\rm Stoner} = \sum_{\langle\alpha,\beta\rangle,\sigma} -t\left(c^+_{\alpha,\sigma}c_{\beta,\sigma} + c^+_{\beta,\sigma}c_{\alpha,\sigma}\right) - h_{\rm ex}\sum_{\alpha}\left(c^+_{\alpha,\uparrow}c_{\alpha,\uparrow} - c^+_{\alpha,\downarrow}c_{\alpha,\downarrow}\right). \quad (2)$$

The case of semi-metal ferromagnets is obtained by considering that the exchange field $h_{\rm ex}$ is larger than the bandwidth D. This model with no minority-spin conduction channel is discussed in Sections 3 and 4. The case of partially polarized ferromagnets corresponding to $h_{\rm ex} < D$ is discussed in Section 3.6.

In the case of half-metal ferromagnets it will be convenient to use the notation

$$t_0 = \frac{t}{\epsilon_{\rm F}}\frac{(a_0k_{\rm F})^2}{4\pi} \quad (3)$$

in which the hopping matrix element is normalized with respect to the Fermi energy. We will use also the notations ρ_0^S for the density of states in the superconductor and $\rho^{\rm F}_\uparrow$ and $\rho^{\rm F}_\downarrow$ for the spin-up and spin-down density of states in the ferromagnetic electrodes:

$$\rho_0^S = \frac{1}{\epsilon_{\rm F}}\frac{(a_0k_{\rm F})^2}{4\pi^2} \quad (4)$$

$$\rho_\uparrow^F = \frac{1}{\epsilon^\uparrow_{\rm F}}\frac{(a_0k^\uparrow_{\rm F})^2}{4\pi^2} \quad (5)$$

$$\rho_\downarrow^F = \frac{1}{\epsilon^\downarrow_{\rm F}}\frac{(a_0k^\downarrow_{\rm F})^2}{4\pi^2}. \quad (6)$$

In the case of ferromagnetic metals with two spin channels (see Sect. 3.6) we will use the dimensionless parameters

$$x_\uparrow = \pi^2t^2\rho_0^S\rho_\uparrow \quad (7)$$

$$x_\downarrow = \pi^2t^2\rho_0^S\rho_\downarrow. \quad (8)$$

2.2 The method

We use a Green's function formalism (see for instance [6,46–49]) to solve the microscopic models given in Section 2.1. The first step is to obtain the expression of the advanced and retarded Green's functions $\hat{G}^{A,R}_{i,j}$ in

terms of the advanced and retarded Green's functions of the disconnected system $\hat{g}^{A,R}_{i,j}$. This is done by solving the Dyson equation

$$\hat{G}^{R,A} = \hat{g}^{R,A} + \hat{g}^{R,A} \otimes \hat{\Sigma} \otimes \hat{G}^{R,A}, \tag{9}$$

where the self-energy $\hat{\Sigma}$ contains all couplings of the tunnel Hamiltonian. The Green's functions of the connected system incorporate all excursions of the electrons in the ferromagnetic electrodes. The convolution in (9) includes a summation over space labels and a convolution of times variables. Since we consider a stationary situation, the latter can be transformed into a product by Fourier transform.

The advanced Green's function takes the following form in the Nambu representation:

$$\hat{g}^{A}_{\alpha,\beta}(t,t') = \\ -\mathrm{i}\theta(t-t') \begin{pmatrix} \langle \left\{ c_{\alpha,\uparrow}(t), c^{+}_{\beta,\uparrow}(t') \right\} \rangle & \langle \{ c_{\alpha,\uparrow}(t), c_{\beta,\downarrow}(t') \} \rangle \\ \langle \left\{ c^{+}_{\alpha,\downarrow}(t), c^{+}_{\beta,\uparrow}(t') \right\} \rangle & \langle \left\{ c^{+}_{\alpha,\downarrow}(t), c_{\beta,\downarrow}(t') \right\} \rangle \end{pmatrix}, \tag{10}$$

where α and β are two arbitrary sites in the superconductor. A similar expression holds for the retarded Green's function. We adopt the following notation for the Nambu components:

$$\hat{g}^{A,R}_{\alpha,\beta}(\omega) = \begin{pmatrix} g^{A,R}_{\alpha,\beta}(\omega) & f^{A,R}_{\alpha,\beta}(\omega) \\ f^{A,R}_{\alpha,\beta}(\omega) & g^{A,R}_{\alpha,\beta}(\omega) \end{pmatrix}.$$

The Nambu representation of the density of states $\hat{\rho}_{\alpha,\beta}(\omega) = \frac{1}{2\mathrm{i}\pi} \left[\hat{g}^{A}_{\alpha,\beta}(\omega) - \hat{g}^{R}_{\alpha,\beta}(\omega) \right]$ will be noted

$$\hat{\rho}_{\alpha,\beta}(\omega) = \begin{pmatrix} \rho^{\alpha,\beta}_{g}(\omega) & \rho^{\alpha,\beta}_{f}(\omega) \\ \rho^{\alpha,\beta}_{f}(\omega) & \rho^{\alpha,\beta}_{g}(\omega) \end{pmatrix},$$

where $\rho^{\alpha,\beta}_{g}(\omega) = \frac{1}{2\mathrm{i}\pi} \left[g^{A}_{\alpha,\beta}(\omega) - g^{R}_{\alpha,\beta}(\omega) \right]$ and $\rho^{\alpha,\beta}_{f}(\omega) = \frac{1}{2\mathrm{i}\pi} \left[g^{A}_{\alpha,\beta}(\omega) - g^{R}_{\alpha,\beta}(\omega) \right]$. Once the advanced and retarded Green's functions has been evaluated using (9), we can evaluate the Keldysh component [46]

$$\hat{G}^{+,-} = \left[\hat{I} + \hat{G}^{R} \otimes \hat{\Sigma} \right] \otimes \hat{g}^{+,-} \otimes \left[\hat{I} + \hat{\Sigma} \otimes \hat{G}^{A} \right], \tag{11}$$

where $\hat{g}^{+,-}_{i,j} = 2\mathrm{i}\pi n_{\mathrm{F}}(\omega - \mu_{i,j})\hat{\rho}_{i,j}$. The Green's function given by (11) can be used either to calculate transport properties (see for instance [47]) or to determine the self consistent value of the superconducting order parameter as we do in the following (see also [1]).

This method can be used to treat non local superconducting pair correlations in the superconductor and in the ferromagnetic electrodes (see Ref. [5]). The pair correlations between two arbitrary sites α and β can be characterized by the non local Gorkov function $\left[G^{+,-}_{\alpha,\beta}(\omega) \right]_{1,2}$. The local Gorkov function $\left[G^{+,-}_{\beta,\beta}(\omega) \right]_{1,2}$ can be used to determine the self consistent value of the superconducting order parameter at any site β in the superconductor (see [50,1]) *via* the self-consistency condition

$$\Delta_{\beta} = -U \int \frac{\mathrm{d}\omega}{2\mathrm{i}\pi} G^{+,-,1,2}_{\beta,\beta}(\omega), \tag{12}$$

where U is the microscopic attractive interaction.

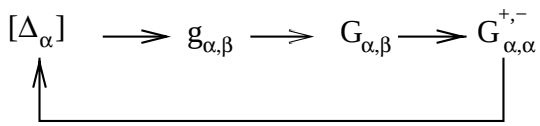

Fig. 1. Representation of the successive operations involved in the calculation of the self consistent value of the superconducting order parameter.

In the following we concentrate on equilibrium properties. Namely, the chemical potentials are identical in all electrodes and there is thus no current flow. In this situation the Keldysh Green's function (11) simplifies into

$$\hat{G}^{+,-}_{\mathrm{eq}} = n_{\mathrm{F}}(\omega - \mu_0) \left(\hat{G}^{A} - \hat{G}^{R} \right), \tag{13}$$

where μ_0 is the chemical potential. The calculations based in (13) will be presented in the main body of the article. In Appendix A we rederive some of our results by using directly equation (11).

The self-consistent value of the superconducting order parameter can be obtained by iterating the process in Figure 1 which starts with a uniform gap profile $[\Delta_\beta]$. From this gap profile we calculate the propagator $g_{\alpha,\beta}(\omega)$ of the superconductor isolated from the ferromagnetic electrodes. From equation (9) we obtain the Green's function $G^{A,R}_{\alpha,\beta}$. From equations (11) or (13) we deduce the Gorkov function $\left[G^{+,-}_{\alpha,\alpha}(\omega) \right]_{1,2}$, which is used to recalculate the superconducting order parameter profile *via* the self consistency equation (12).

2.3 The different approaches used to determine the self consistent gap profile

2.3.1 Position of the problem

To discuss F/S/F trilayers we need to find reliable determinations of the self consistent order parameter. It is in practice impossible to make an exact analytical calculation of the self consistent order parameter except in the limit already considered in reference [45] where the superconducting gap is uniform in space (the superconductor is smaller than the coherence length). The reason why we cannot find exact solutions is the following. Let us start with a uniform gap profile $\Delta_\beta \equiv \Delta_0$ and consider the successive operations in Figure 1. Because of the contacts between the superconductor and the ferromagnetic electrodes, the Green's functions $G^{R,A}_{\alpha,\beta}$ are not translational invariant. As a result in the next iteration, the superconducting order parameter is not translational

invariant. The expression of the propagators of an isolated superconductor in the presence of a non uniform superconducting order parameter is not known in general. The self consistency relation (12) is thus a functional relation:

$$\Delta_\beta = -U \int \frac{\mathrm{d}\omega}{2\mathrm{i}\pi} G^{+,-,1,2}_{\beta,\beta}\left([\Delta],\omega\right), \tag{14}$$

where the notation $[\Delta]$ means that the right hand side depends on all values of the gap profile. As a consequence, we cannot find exact solutions for the gap profile.

2.3.2 Local approach

We present in Section 3 an approximate analytical treatment in which the functional self consistency relation (14) is replaced by a local relation:

$$\Delta_\beta = -U \int \frac{\mathrm{d}\omega}{2\mathrm{i}\pi} G^{+,-,1,2}_{\beta,\beta}(\Delta_\beta,\omega)\cdot \tag{15}$$

To transform (14) into (15), we assume that the propagators of the isolated superconductor in the presence of a non uniform gap has the same energy dependence as the propagators with a uniform gap. The propagators $g^{A,R}_{\alpha,\beta}$ and $f^{A,R}_{\alpha,\beta}$ depend on an effective gap $\Delta_{\alpha,\beta}$.

2.3.3 Exact diagonalizations

We present in Section 4 another possible approach in which we use exact diagonalizations to solve exactly the functional form of the self consistency equation (14). This numerical method is restricted to small system sizes. We will find that the exact diagonalizations are consistent with the "local" approach in Section 3 in the sense that we find $\Delta_{\mathrm{AF}} < \Delta_{\mathrm{F}}$ with both approaches for metallic ferromagnets.

2.4 Green's functions in the presence of a uniform superconducting order parameter

We end-up this preliminary section by giving the form of the Green's function of a superconductor having a uniform superconducting order parameter: $\Delta_\beta \equiv \Delta_0$ for all sites β. The spectral representation has already been given in reference [6], as well as the final form of the propagators below the superconducting gap. The final form of the propagators above the superconducting gap is found to be

$$\begin{aligned}\hat{g}^{R,A}_{\alpha,\beta}(\omega) = \frac{ma_0^3}{\hbar^2}\frac{1}{2\pi|\mathbf{x}_\alpha-\mathbf{x}_\beta|}\exp\left[\mp\mathrm{i}\psi(\omega)\right]\\ \times\left\{\frac{\mp\mathrm{i}\sin\varphi}{\sqrt{(\omega-\mu_S)^2-\Delta^2_{\alpha,\beta}}}\right.\\ \left.\times\begin{bmatrix}-(\omega-\mu_S) & \Delta_{\alpha,\beta}\\ \Delta_{\alpha,\beta} & -(\omega-\mu_S)\end{bmatrix}-\cos\varphi\begin{bmatrix}1&0\\0&1\end{bmatrix}\right\},\end{aligned} \tag{16}$$

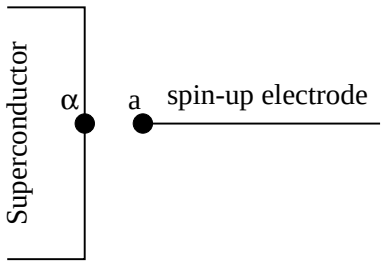

Fig. 2. Representation of a model in which a single channel spin-up electrode is in contact with a superconductor.

where the phase in the prefactor is given by

$$\psi(\omega) = \frac{1}{v_{\mathrm{F}}}|\mathbf{x}_\alpha-\mathbf{x}_\beta|\sqrt{(\omega-\mu_S)^2-\Delta^2_{\alpha,\beta}}, \tag{17}$$

and $\varphi(\omega) = k_{\mathrm{F}}|\mathbf{x}_\alpha-\mathbf{x}_\beta|$. If $\omega \gg \Delta$, the Green's function reduces to

$$g^A_{\alpha,\beta}(\omega) = -\frac{ma_0^3}{\hbar^2}\frac{1}{2\pi R_{\alpha,\beta}}\exp\left[\mathrm{i}\left(\psi(\omega)+\varphi(\omega)\right)\right],$$

which will be used in Section 3.4.

3 Half-metal ferromagnets and ferromagnets with both spin channels: analytical results

We discuss in this section mainly the solutions of F/S/F trilayers with half-metal ferromagnets having a single spin conduction channel. In Section 3.6 we extend our discussion to a model having both spin conduction channels. As discussed in Section 2.3.1, the self-consistency equation for the superconducting order parameter (14) is a functional of the gap profile. In this section, we replace the functional equation (14) by the local equation (15).

3.1 Superconductor connected to a single-channel half-metal ferromagnet

We first consider the case in Figure 2 where a superconductor is connected to a single-channel half-metal ferromagnetic electrode. Using the Dyson equation (9) and the expression (13) of the equilibrium Gorkov function, we obtain easily the local Gorkov function

$$\begin{aligned}G^{+,-}_{\beta,\beta} = 2\mathrm{i}\pi n_{\mathrm{F}}(\omega)\left\{\rho_f^{\beta,\beta}+\frac{|t_{a,\alpha}|^2}{2\mathrm{i}\pi}\left[\frac{1}{\mathcal{D}^{\mathcal{A}}}g^{a,a,A}_{1,1}g^{\beta,\alpha,A}f^{\alpha,\beta,A}\right.\right.\\ \left.\left.-\frac{1}{\mathcal{D}^{\mathcal{R}}}g^{a,a,R}_{1,1}g^{\beta,\alpha,R}f^{\alpha,\beta,R}\right]\right\},\end{aligned} \tag{18}$$

with

$$\mathcal{D} = 1-|t^{a,\alpha}|^2 g^{a,a}_{1,1}g^{\alpha,\alpha}. \tag{19}$$

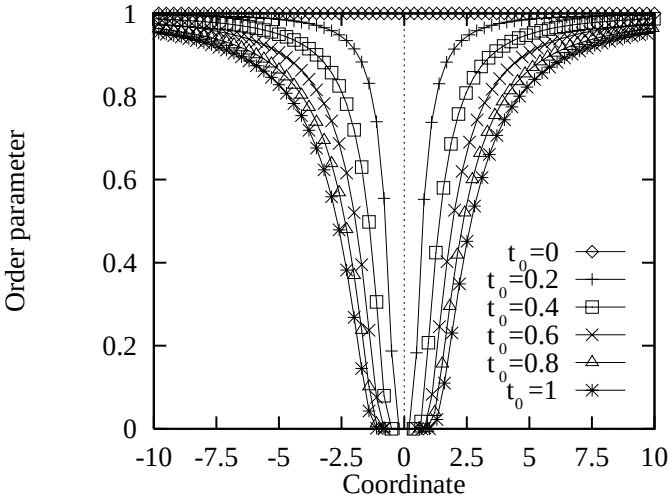

Fig. 3. Variation of the superconducting order parameter with a single ferromagnetic channel. We used realistic parameters: the Fermi energy is $\epsilon_{\rm F} = 10$ eV and the value of the attractive electron – electron interaction is such that the bulk superconducting order parameter is $\Delta_{\rm bulk} = 1$ meV.

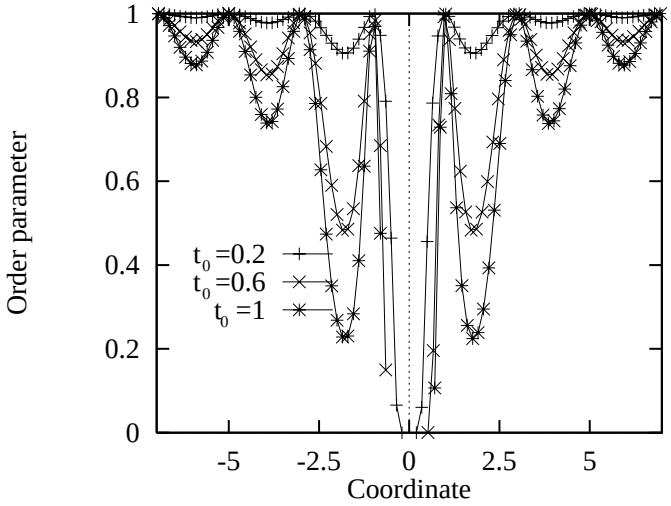

Fig. 4. Variation of the superconducting order parameter as a function of the distance to the contact in the case of a superconductor connected to a single-channel ferromagnetic electrode. We have incorporated the oscillatory phase factor in (21) and we suppose that $k_{\rm F}a_0 = \frac{\pi}{2}$. The period of the oscillations is thus $2a_0$, as expected for $2k_{\rm F}$ oscillations. The parameters are the same as in Figure 3.

3.1.1 Gap profile with fixed phases

We first make the additional assumption that the electronic phase in the Green's function (16) does not depend on distance: $\varphi = -\pi/2$ for all distances. Phase averaging will be discussed in Section 3.4. The gap profile is found to be

$$\Delta_\beta = 2D \exp\left\{-\frac{1}{U}\frac{2\pi^2\hbar^2}{ma_0^2}\left[1-\left(\frac{a_0}{R_{\alpha,\beta}}\right)^2\frac{t_0^2}{1+t_0^2}\right]^{-1}\right\}, \tag{20}$$

where t_0 is given by equation (3). $R_{\alpha,\beta} = |\mathbf{x}_\alpha - \mathbf{x}_\beta|$ is the distance between sites α and β in the superconductor. Far away from the contact the superconducting order parameter is equal to the bulk value. The minimum value of the superconducting order parameter at the contact can be estimated from equation (20) by replacing $R_{\alpha,\beta}$ by the lattice spacing a_0:

$$\Delta_\alpha = 2D \exp\left\{-\frac{1}{U}\frac{2\pi^2\hbar^2}{ma_0^2}\left[1+t_0^2\right]\right\}.$$

The complete gap profile is shown in Figure 3 for several values of the hopping between the superconductor and the ferromagnetic channel.

3.1.2 Role of $2k_{\rm F}$ oscillations

Now we discuss the role played by the phase φ appearing in the Green's function $g_{\alpha,\beta}$ (see Eq. (16)). In the presence of this phase factor, the self consistent superconducting order parameter develops $2k_{\rm F}$ oscillations:

$$\Delta_\beta = 2D \exp\left\{-\frac{1}{U}\frac{2\pi^2\hbar^2}{ma_0^2} \times \left[1-\left(\frac{a_0}{R_{\alpha,\beta}}\right)^2\frac{t_0^2}{1+t_0^2}\sin^2\left(k_{\rm F}R_{\alpha,\beta}\right)\right]^{-1}\right\}, \tag{21}$$

where $R_{\alpha,\beta} = |\mathbf{x}_\alpha - \mathbf{x}_\beta|$. The gap profile is shown in Figure 4. One may notice that $\Delta_{\rm bulk} - \Delta(R_{\alpha,\beta})$ deduced from Figure 4 is related to the wave function of a spin-up electron injected at site α in the superconductor. Namely the superconducting gap is maximal when the spin-up wave function is minimal.

3.2 Superconductor connected to two single-channel half-metal ferromagnets

Now we consider that two single-channel half-metal ferromagnets are connected to a superconductor (see Fig. 5). We assume that the electronic phases are fixed to the value $\varphi = -\pi/2$ for all distances and postpone for Section 3.4 the discussion of phase averaging.

3.2.1 Antiferromagnetic alignment

Let us consider the model in Figure 5 in which two single-channel half-metal spin-up and spin-down electrodes are in

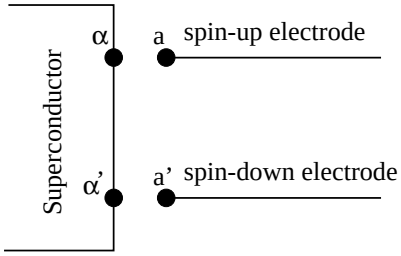

Fig. 5. The model in which two single channel half-metal electrodes are in contact with a superconductor.

contact with a superconductor. The local Green's function takes the form

$$\hat{G}^{\beta,\beta} = \hat{g}^{\beta,\beta} + \hat{g}^{\beta,\alpha}\hat{t}^{\alpha,a}\hat{G}^{a,\beta} + \hat{g}^{\beta,\alpha'}\hat{t}^{\alpha',a'}\hat{G}^{a',\beta}. \quad (22)$$

The propagators $\hat{G}^{a,\beta}$ and $\hat{G}^{a',\beta}$ are given by

$$\hat{G}^{a,\beta} = t^{a,\alpha} g^{a,a}_{1,1} \begin{bmatrix} \tilde{g}^{\alpha,\beta} & \tilde{f}^{\alpha,\beta} \\ 0 & 0 \end{bmatrix} \quad (23)$$

$$\hat{G}^{a',\beta} = -t^{a',\alpha'} g^{a',a'}_{2,2} \begin{bmatrix} 0 & 0 \\ \tilde{f}^{\alpha',\beta} & \tilde{g}^{\alpha',\beta} \end{bmatrix}, \quad (24)$$

where

$$\tilde{g}^{\alpha,\beta} = \frac{1}{\mathcal{D}_{\rm AF}} \left[g^{\alpha,\beta} + |t^{a',\alpha'}|^2 g^{a',a'}_{2,2} \left(f^{\alpha,\alpha'} f^{\alpha'\beta} - g^{\alpha',\alpha'} g^{\alpha,\beta} \right) \right] \quad (25)$$

$$\tilde{f}^{\alpha,\beta} = \frac{1}{\mathcal{D}_{\rm AF}} \left[f^{\alpha,\beta} + |t^{a',\alpha'}|^2 g^{a',a'}_{2,2} \left(f^{\alpha,\alpha'} g^{\alpha',\beta} - g^{\alpha',\alpha'} f^{\alpha,\beta} \right) \right], \quad (26)$$

and where

$$\mathcal{D}_{\rm AF} = \left[1 - |t^{a,\alpha}|^2 g^{a,a}_{1,1} g^{\alpha,\alpha}\right] \left[1 - |t^{a',\alpha'}|^2 g^{a',a'}_{2,2} g^{\alpha',\alpha'}\right] - |t^{a,\alpha}|^2 |t^{a',\alpha'}|^2 g^{a,a}_{1,1} g^{a',a'}_{2,2} f^{\alpha,\alpha'} f^{\alpha',\alpha}. \quad (27)$$

The self-consistent superconducting order parameter is obtained by evaluating the high energy behavior of the local Gorkov function given by (13). We use a "local" approximation in which the gaps $\Delta_{\alpha,\beta}$ and $\Delta_{\alpha',\beta}$ appearing in the propagators $g_{\alpha,\beta}$ and $f_{\alpha,\beta}$ are replaced by the local gap Δ_β. The high energy behavior of the local Gorkov is found to be

$$\hat{G}^{+,-}_{\beta,\beta} = -2{\rm i}\pi n_{\rm F}(\omega) \frac{m a_0^2}{2\pi^2\hbar^2} \left(\frac{\Delta_\beta}{\omega}\right) \Lambda^{\rm AF}_{\rm Metal}, \quad (28)$$

with

$$\Lambda^{\rm AF}_{\rm Metal} = 1 - \frac{a_0^2}{R^2_{\alpha,\beta}} \left(\frac{|t_0^{a,\alpha}|^2}{1+|t_0^{a,\alpha}|^2} \right) - \frac{a_0^2}{R^2_{\alpha',\beta}} \left(\frac{|t_0^{a',\alpha'}|^2}{1+|t_0^{a',\alpha'}|^2} \right) + \frac{a_0^3}{R_{\alpha,\beta}R_{\alpha',\beta}R_{\alpha,\alpha'}} \left(\frac{|t_0^{a,\alpha}|^2}{1+|t_0^{a,\alpha}|^2} \right) \left(\frac{|t_0^{a',\alpha'}|^2}{1+|t_0^{a',\alpha'}|^2} \right), \quad (29)$$

where $t_0^{a,\alpha}$ and $t_0^{a',\alpha'}$ are the tunnel matrix elements normalized to the Fermi energy (see Eq. (3)).

3.2.2 Ferromagnetic alignment

Using the same method for the ferromagnetic alignment, we obtain the high energy behavior of the local Gorkov function

$$\hat{G}^{+,-}_{\beta,\beta} = -2{\rm i}\pi n_{\rm F}(\omega) \frac{m a_0^2}{2\pi^2\hbar^2} \left(\frac{\Delta_\beta}{\omega}\right) \Lambda^{\rm F}_{\rm Metal}, \quad (30)$$

with

$$\Lambda^{\rm F}_{\rm Metal} = 1 - \frac{a_0^2}{R^2_{\alpha,\beta}} \left(\frac{|t_0^{a,\alpha}|^2}{1+|t_0^{a,\alpha}|^2} \right) - \frac{a_0^2}{R^2_{\alpha',\beta}} \left(\frac{|t_0^{a',\alpha'}|^2}{1+|t_0^{a',\alpha'}|^2} \right) + 2|t_0^{a,\alpha}|^2 |t_0^{a',\alpha'}|^2 \frac{1}{\mathcal{D}_{\rm F}} \frac{a_0^3}{R_{\alpha,\beta}R_{\alpha',\beta}R_{\alpha,\alpha'}}, \quad (31)$$

and

$$\mathcal{D}_{\rm F} = \left[1 - |t^{a,\alpha}|^2 g^{a,a}_{1,1} g^{\alpha,\alpha}\right] \left[1 - |t^{a',\alpha'}|^2 g^{a',a'}_{2,2} g^{\alpha',\alpha'}\right] - |t^{a,\alpha}|^2 |t^{a',\alpha'}|^2 g^{a,a}_{1,1} g^{a',a'}_{2,2} g^{\alpha,\alpha'} g^{\alpha',\alpha}. \quad (32)$$

To order $1/R^3$, equation (31) becomes

$$\Lambda^{\rm F}_{\rm Metal} = 1 - \frac{a_0^2}{R^2_{\alpha,\beta}} \left(\frac{|t_0^{a,\alpha}|^2}{1+|t_0^{a,\alpha}|^2} \right) - \frac{a_0^2}{R^2_{\alpha',\beta}} \left(\frac{|t_0^{a',\alpha'}|^2}{1+|t_0^{a',\alpha'}|^2} \right) + 2\frac{a_0^3}{R_{\alpha,\beta}R_{\alpha',\beta}R_{\alpha,\alpha'}} \left(\frac{|t_0^{a,\alpha}|^2}{1+|t_0^{a,\alpha}|^2} \right) \left(\frac{|t_0^{a',\alpha'}|^2}{1+|t_0^{a',\alpha'}|^2} \right). \quad (33)$$

Comparing equations (29) and (33), we see that:

(i) As expected, the "local" contributions of order $1/R^2_{\alpha,\beta}$ and $1/R^2_{\alpha',\beta}$ do not depend on the relative spin orientation of the ferromagnetic electrodes. The local contributions generate a reduction of the superconducting order parameter.

(ii) The lowest order "non local" contribution arises at order $1/[R_{\alpha,\beta}R_{\alpha',\beta}R_{\alpha,\alpha'}]$, and depends on the relative spin orientation of the ferromagnetic electrodes *via* a factor of two in equation (33), not present in equation (29). Because of this non local contribution, the superconducting gap is larger in the ferromagnetic alignment, which can receive a simple interpretation in terms of the diagrams contributing to this non local term (see Sect. 3.5).

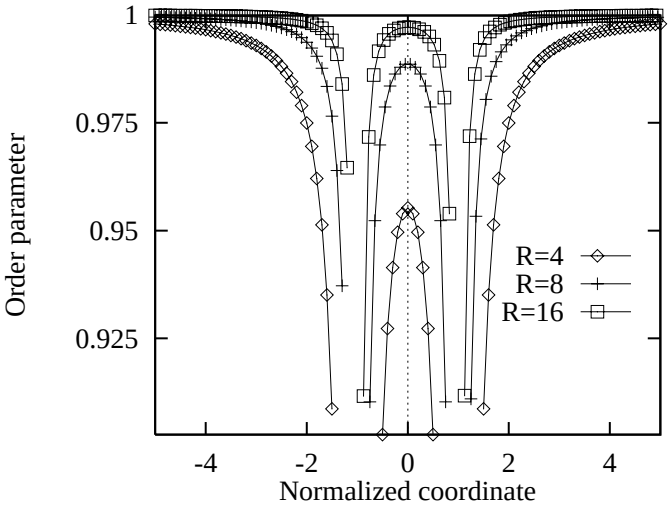

Fig. 6. Variation of the superconducting order parameter in the presence of two ferromagnetic electrodes. It is assumed that the point β is aligned with the points α and α'. The coordinate is normalized to the separation $R_{\alpha,\alpha'}$ between the contacts. The different curves correspond to $R_{\alpha,\alpha'} = 4$ ($\Diamond$), $R_{\alpha,\alpha'} = 8$ (+) and $R_{\alpha,\alpha'} = 16$ ($\Box$). We used the same parameters as in Figure 3. The contacts have a low transparency: $t_0^{a,\alpha} = t_0^{a',\alpha'} = 0.1$. The ferromagnetic electrodes have an antiparallel spin orientation.

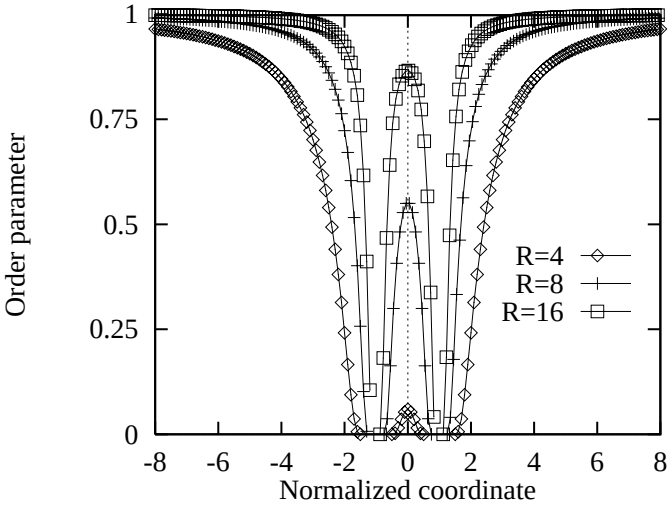

Fig. 7. The same as Figure 7 with high transparency contacts: $t_0^{a,\alpha} = t_0^{a',\alpha'} = 1$.

3.2.3 Gap profiles

The gap profiles are shown in Figure 6 in the tunnel regime and Figure 7 in the high transparency regime. The gap is reduced close to the contacts with the ferromagnets, which was already obtained for the single channel model in Sections 3.1 and 3.1.2 (see Figs. 3 and 4).

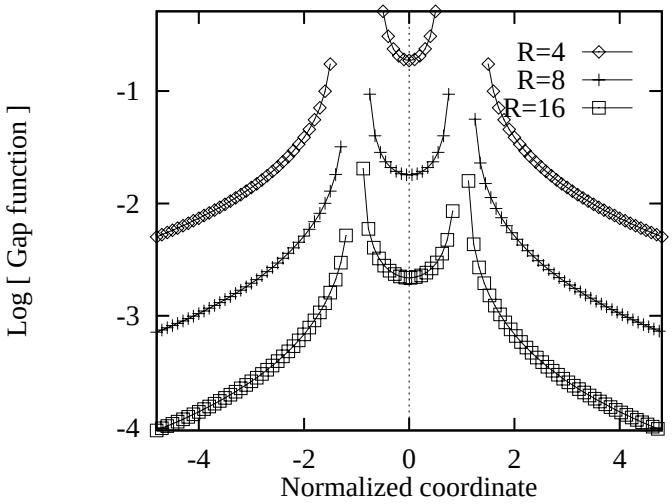

Fig. 8. Variation of the logarithm of δ_β defined by (34). The ferromagnetic gap is larger than the antiferromagnetic gap. The parameters are the same as in Figure 3. The contacts have a high transparency: $t_0^{a,\alpha} = t_0^{a',\alpha'} = 1$.

3.2.4 Difference between the superconducting gaps in the ferromagnetic and antiferromagnetic alignments

At each point β in the superconductor, we define δ_β as

$$\delta_\beta = 2\frac{\Delta_\beta^{\rm F} - \Delta_\beta^{\rm AF}}{\Delta_\beta^{\rm F} + \Delta_\beta^{\rm AF}} \cdot \tag{34}$$

δ_β is positive for metallic ferromagnets, and takes a simple form at large distance:

$$\delta_\beta \simeq \frac{1}{U}\frac{2\pi^2\hbar^2}{ma_0^2}\frac{|t_0^{a,\alpha}|^2}{1+|t_0^{a,\alpha}|^2}\frac{|t_0^{a',\alpha'}|^2}{1+|t_0^{a',\alpha'}|^2}\frac{a_0^3}{R_{\alpha,\beta}R_{\alpha',\beta}R_{\alpha,\alpha'}} \cdot \tag{35}$$

The variations of δ_β are shown in Figure 8.

3.3 Superconductor connected to two single-channel insulating ferromagnets

Now we show that we recover the correct physics in the case of insulating ferromagnets [42]. The propagator relevant to describe a ferromagnetic insulator decays exponentially with distance and is such that $g_{i,j}^A = g_{i,j}^R$. The local propagators $g_{a,a}$ and $g_{a',a'}$ are real numbers. Using the same method as in Section 3.2 we find that the Gorkov functions are still given by (28) and (30) but with a different form of $\Lambda^{\rm AF}$ and $\Lambda^{\rm F}$. The expression of the Gorkov functions to order $1/R^3$ is the following:

$$\begin{aligned}\Lambda_{\rm Ins}^{\rm AF} = 1 &- \frac{a_0^2}{R_{\alpha,\beta}^2}\left(\frac{|t_0^{a,\alpha}|^4}{1+|t_0^{a,\alpha}|^4}\right) - \frac{a_0^2}{R_{\alpha',\beta}^2}\left(\frac{|t_0^{a',\alpha'}|^4}{1+|t_0^{a',\alpha'}|^4}\right)\\ &- \frac{a_0^3}{R_{\alpha,\beta}R_{\alpha',\beta}R_{\alpha,\alpha'}}\left(1-|t_0^{a,\alpha}|^2|t_0^{a',\alpha'}|^2\right)\\ &\times\left(\frac{|t_0^{a,\alpha}|^2}{1+|t_0^{a,\alpha}|^4}\right)\left(\frac{|t_0^{a',\alpha'}|^2}{1+|t_0^{a',\alpha'}|^4}\right)\end{aligned} \tag{36}$$

$$\Lambda_{\rm Ins}^{\rm F} = 1 - \frac{a_0^2}{R_{\alpha,\beta}^2}\left(\frac{|t_0^{a,\alpha}|^4}{1+|t_0^{a,\alpha}|^4}\right) - \frac{a_0^2}{R_{\alpha',\beta}^2}\left(\frac{|t_0^{a',\alpha'}|^4}{1+|t_0^{a',\alpha'}|^4}\right) - 2\frac{a_0^3}{R_{\alpha,\beta}R_{\alpha',\beta}R_{\alpha,\alpha'}}\left(1-|t_0^{a,\alpha}|^2|t_0^{a',\alpha'}|^2\right) \times \left(\frac{|t_0^{a,\alpha}|^2}{1+|t_0^{a,\alpha}|^4}\right)\left(\frac{|t_0^{a',\alpha'}|^2}{1+|t_0^{a',\alpha'}|^4}\right). \quad (37)$$

We deduce from (36) and (37) the value of δ_β defined by (34):

$$\delta_\beta = -\frac{1}{U}\frac{2\pi^2\hbar^2}{ma_0^2}\left(1-|t_0^{a,\alpha}|^2|t_0^{a',\alpha'}|^2\right) \times \frac{|t_0^{a,\alpha}|^2}{1+|t_0^{a,\alpha}|^4}\frac{|t_0^{a',\alpha'}|^2}{1+|t_0^{a',\alpha'}|^4}\frac{a_0^3}{R_{\alpha,\beta}R_{\alpha',\beta}R_{\alpha,\alpha'}}.$$

The values of the normalized tunnel matrix elements are such that $|t_0^{a,\alpha}||t_0^{a',\alpha'}| < 1$. As a consequence we recover the perturbative result obtained in reference [42] for insulating ferromagnets ($\delta_\beta < 0$).

3.4 Phase averaging

The microscopic Green's function $\hat{g}^{\alpha,\beta}$ depends on the phase variables $\varphi_{\alpha,\beta}(\omega)$ and $\psi_{\alpha,\beta}(\omega)$ (see Eq. (16)). In the preceding subsections, we have assumed that these phases were fixed to $\varphi_{\alpha,\beta}(\omega) = -\pi/2$ and $\psi_{\alpha,\beta}(\omega) = 0$ for all distances. In fact the microscopic phases phases given by (17) oscillate rapidly on microscopic scales, as opposed to the slowly varying prefactor involving $1/R_{\alpha,\beta}$ in $\hat{g}_{\alpha,\beta}$ (see Eq. (16)). Moreover in a multichannel model these phases are averaged out when the summation over all channels is carried out (see Ref. [6]). It is thus legitimate to consider the phases as random variables and to average the Gorkov functions over "phase disorder".

3.4.1 Single-channel problem

Let us start with the single-channel problem in Figure 2. The local Gorkov function were already given in equation (18). We need to evaluate $\langle\langle g^{\beta,\alpha,A} f^{\alpha,\beta,A}\rangle\rangle$ and $\langle\langle g^{\beta,\alpha,R} f^{\alpha,\beta,R}\rangle\rangle$, where $\langle\langle\ \rangle\rangle$ denotes the averaging over phase disorder. Assuming that the phases are symmetric (namely $\varphi_{\alpha,\beta}(\omega) = \varphi_{\beta,\alpha}(\omega)$ and $\psi_{\alpha,\beta}(\omega) = \psi_{\beta,\alpha}(\omega)$) leads to $\langle\langle g^{\beta,\alpha,A} f^{\alpha,\beta,A}\rangle\rangle = 0$ and $\langle\langle g^{\beta,\alpha,R} f^{\alpha,\beta,R}\rangle\rangle = 0$, from what we deduce that the superconducting gap does not depend on the transparency of the contact with the ferromagnet. Since this conclusion is not acceptable physically, we suppose instead that the phases are antisymmetric: $\varphi_{\alpha,\beta} = -\pi/2 + k_{\rm F}R_{\alpha,\beta}$, $\varphi_{\beta,\alpha} = -\pi/2 - k_{\rm F}R_{\alpha,\beta}$, and $\psi_{\alpha,\beta} = -\psi_{\beta,\alpha}$. Then the expectation value of $\langle\langle g^{\beta,\alpha,A} f^{\alpha,\beta,A}\rangle\rangle$ is finite, as it should:

$$\langle\langle g^{\beta,\alpha,A} f^{\alpha,\beta,A}\rangle\rangle = \frac{1}{2}\left(\frac{ma_0^2}{2\pi^2\hbar^2}\right)\left(\frac{a_0}{R_{\alpha,\beta}}\right)^2\frac{\Delta_0}{\sqrt{\omega^2-\Delta_0^2}}, \quad (38)$$

from what we deduce the self consistent superconducting order parameter

$$\Delta_\beta = 2D\exp\left\{-\frac{1}{U}\frac{2\pi^2\hbar^2}{ma_0^2}\left[1-\frac{1}{2}\left(\frac{a_0}{R_{\alpha,\beta}}\right)^2\frac{t_0^2}{1+t_0^2}\right]^{-1}\right\}. \quad (39)$$

This form of the gap profile is similar to equation (20), except for the coefficient 1/2 due to phase averaging. Now we discuss phase averaging in different types of two-channel heterostructures.

3.4.2 Superconductor connected to two single-channel half-metal ferromagnets

With two half-metal ferromagnets, we obtain

$$\Lambda_{\rm Metal}^{\rm AF} = 1 - \frac{a_0^2}{R_{\alpha,\beta}^2}\left(\frac{|t_0^{a,\alpha}|^2}{1+|t_0^{a,\alpha}|^2}\right)\sin^2(\varphi_{\alpha,\beta}) - \frac{a_0^2}{R_{\alpha',\beta}^2}\left(\frac{|t_0^{a',\alpha'}|^2}{1+|t_0^{a',\alpha'}|^2}\right)\sin^2(\varphi_{\alpha',\beta}) + \frac{a_0^3}{R_{\alpha,\beta}R_{\alpha',\beta}R_{\alpha,\alpha'}}\left(\frac{|t_0^{a,\alpha}|^2}{1+|t_0^{a,\alpha}|^2}\right) \times \left(\frac{|t_0^{a',\alpha'}|^2}{1+|t_0^{a',\alpha'}|^2}\right)\sin(\varphi_{\alpha,\alpha'})\cos(\varphi_{\beta,\alpha}+\varphi_{\alpha',\beta}) \quad (40)$$

$$\Lambda_{\rm Metal}^{\rm F} = 1 - \frac{a_0^2}{R_{\alpha,\beta}^2}\left(\frac{|t_0^{a,\alpha}|^2}{1+|t_0^{a,\alpha}|^2}\right)\sin^2(\varphi_{\alpha,\beta}) - \frac{a_0^2}{R_{\alpha',\beta}^2}\left(\frac{|t_0^{a',\alpha'}|^2}{1+|t_0^{a',\alpha'}|^2}\right)\sin^2(\varphi_{\alpha',\beta}) + \frac{a_0^3}{R_{\alpha,\beta}R_{\alpha',\beta}R_{\alpha,\alpha'}}\left(\frac{|t_0^{a,\alpha}|^2}{1+|t_0^{a,\alpha}|^2}\right) \times \left(\frac{|t_0^{a',\alpha'}|^2}{1+|t_0^{a',\alpha'}|^2}\right)\{\cos(\varphi_{\beta,\alpha}+\varphi_{\alpha,\alpha'})\sin(\varphi_{\alpha',\beta}) + \cos(\varphi_{\beta,\alpha'}+\varphi_{\alpha',\alpha})\sin(\varphi_{\alpha,\beta})\}. \quad (41)$$

After averaging over phase disorder, we find

$$\langle\langle\Lambda_{\rm Metal}^{\rm AF}\rangle\rangle = 1 - \frac{1}{2}\frac{a_0^2}{R_{\alpha,\beta}^2}\left(\frac{|t_0^{a,\alpha}|^2}{1+|t_0^{a,\alpha}|^2}\right) - \frac{1}{2}\frac{a_0^2}{R_{\alpha',\beta}^2}\left(\frac{|t_0^{a',\alpha'}|^2}{1+|t_0^{a',\alpha'}|^2}\right) + \frac{1}{2}\frac{a_0^3}{R_{\alpha,\beta}R_{\alpha',\beta}R_{\alpha,\alpha'}}\left(\frac{|t_0^{a,\alpha}|^2}{1+|t_0^{a,\alpha}|^2}\right)\left(\frac{|t_0^{a',\alpha'}|^2}{1+|t_0^{a',\alpha'}|^2}\right) \quad (42)$$

$$\langle\langle\Lambda_{\rm Metal}^{\rm F}\rangle\rangle = 1 - \frac{1}{2}\frac{a_0^2}{R_{\alpha,\beta}^2}\left(\frac{|t_0^{a,\alpha}|^2}{1+|t_0^{a,\alpha}|^2}\right) - \frac{1}{2}\frac{a_0^2}{R_{\alpha',\beta}^2}\left(\frac{|t_0^{a',\alpha'}|^2}{1+|t_0^{a',\alpha'}|^2}\right) + \frac{a_0^3}{R_{\alpha,\beta}R_{\alpha',\beta}R_{\alpha,\alpha'}}\left(\frac{|t_0^{a,\alpha}|^2}{1+|t_0^{a,\alpha}|^2}\right)\left(\frac{|t_0^{a',\alpha'}|^2}{1+|t_0^{a',\alpha'}|^2}\right). \quad (43)$$

The form of the Gorkov functions is therefore similar to equations (29, 33), except for the 1/2 prefactors.

3.4.3 Superconductor connected to two single-channel insulating ferromagnets

For a superconductor connected to two insulating ferromagnets, we obtain

$$\langle\langle \Lambda^{\rm AF}_{\rm Ins}\rangle\rangle = 1 - \frac{1}{2}\frac{a_0^2}{R^2_{\alpha,\beta}}\left(\frac{|t_0^{a,\alpha}|^4}{1+|t_0^{a,\alpha}|^4}\right) - \frac{1}{2}\frac{a_0^2}{R^2_{\alpha',\beta}}\left(\frac{|t_0^{a',\alpha'}|^4}{1+|t_0^{a',\alpha'}|^4}\right) - \frac{1}{2}\frac{a_0^3}{R_{\alpha,\beta}R_{\alpha',\beta}R_{\alpha,\alpha'}}\left(1-|t_0^{a,\alpha}|^2|t_0^{a',\alpha'}|^2\right) \times \left(\frac{|t_0^{a,\alpha}|^2}{1+|t_0^{a,\alpha}|^4}\right)\left(\frac{|t_0^{a',\alpha'}|^2}{1+|t_0^{a',\alpha'}|^4}\right) \quad (44)$$

$$\langle\langle \Lambda^{\rm F}_{\rm Ins}\rangle\rangle = 1 - \frac{1}{2}\frac{a_0^2}{R^2_{\alpha,\beta}}\left(\frac{|t_0^{a,\alpha}|^4}{1+|t_0^{a,\alpha}|^4}\right) - \frac{1}{2}\frac{a_0^2}{R^2_{\alpha',\beta}}\left(\frac{|t_0^{a',\alpha'}|^4}{1+|t_0^{a',\alpha'}|^4}\right) - \frac{a_0^3}{R_{\alpha,\beta}R_{\alpha',\beta}R_{\alpha,\alpha'}}\left(1-|t_0^{a,\alpha}|^2|t_0^{a',\alpha'}|^2\right) \times \left(\frac{|t_0^{a,\alpha}|^2}{1+|t_0^{a,\alpha}|^4}\right)\left(\frac{|t_0^{a',\alpha'}|^2}{1+|t_0^{a',\alpha'}|^4}\right), \quad (45)$$

which differs from (36) and (37) by the 1/2 coefficients.

3.4.4 "Mixed" junction with an insulating and a metallic single-channel ferromagnet

Now we consider the "mixed" heterostructure in Figure 5 in which electrode "a" is a single-channel half metal ferromagnet and electrode "b" is insulating. Using the same formalism as in the preceding sections, we obtain

$$\begin{aligned}\Lambda^{\rm AF}_{\rm Mixed} = {} & 1 - \frac{a_0^2}{R^2_{\alpha,\beta}}\left(\frac{|t_0^{a,\alpha}|^2}{1+|t_0^{a,\alpha}|^2}\right)\sin^2(\varphi_{\alpha,\beta}) \\ & + \frac{a_0^2}{R^2_{\alpha',\beta}}\left(\frac{|t_0^{a',\alpha'}|^2}{1+|t_0^{a',\alpha'}|^4}\right)\sin(\varphi_{\beta,\alpha'}) \\ & \times\Big[\cos(\varphi_{\alpha'\beta}) - |t_0^{a',\alpha'}|^2\sin(\varphi_{\alpha',\beta})\Big] \\ & + \frac{a_0^3}{R_{\alpha,\beta}R_{\alpha',\beta}R_{\alpha,\alpha'}}\left(\frac{|t_0^{a,\alpha}|^2}{1+|t_0^{a,\alpha}|^2}\right)\left(\frac{|t_0^{a',\alpha'}|^2}{1+|t_0^{a',\alpha'}|^4}\right) \\ & \times\sin(\varphi_{\alpha,\alpha'})\big[\sin(\varphi_{\beta,\alpha}+\varphi_{\alpha',\beta}) + |t_0^{a',\alpha'}|^2 \\ & \times\cos(\varphi_{\beta,\alpha}+\varphi_{\alpha',\beta})\big] \end{aligned} \quad (46)$$

$$\begin{aligned}\Lambda^{\rm F}_{\rm Mixed} = {} & 1 - \frac{a_0^2}{R^2_{\alpha,\beta}}\left(\frac{|t_0^{a,\alpha}|^2}{1+|t_0^{a,\alpha}|^2}\right)\sin^2(\varphi_{\alpha,\beta}) \\ & + \frac{a_0^2}{R^2_{\alpha',\beta}}\left(\frac{|t_0^{a',\alpha'}|^2}{1+|t_0^{a',\alpha'}|^4}\right)\Big[\cos(\varphi_{\beta,\alpha'})\sin(\varphi_{\alpha',\beta}) \\ & - |t_0^{a',\alpha'}|^2\sin(\varphi_{\alpha',\beta})\sin(\varphi_{\beta,\alpha'})\Big] \\ & + \frac{a_0^3}{R_{\alpha,\beta}R_{\alpha',\beta}R_{\alpha,\alpha'}}\left(\frac{|t_0^{a,\alpha}|^2}{1+|t_0^{a,\alpha}|^2}\right)\left(\frac{|t_0^{a',\alpha'}|^2}{1+|t_0^{a',\alpha'}|^4}\right) \\ & \times\Big[\sin(\varphi_{\beta,\alpha}+\varphi_{\alpha,\alpha'})\sin(\varphi_{\alpha',\beta}) \\ & + \sin(\varphi_{\beta,\alpha'}+\varphi_{\alpha',\alpha})\sin(\varphi_{\alpha,\beta}) \\ & + |t_0^{a',\alpha'}|^2\left(\cos(\varphi_{\beta,\alpha}+\varphi_{\alpha,\alpha'})\sin(\varphi_{\alpha',\beta})\right. \\ & \left. + \cos(\varphi_{\beta,\alpha'}+\varphi_{\alpha',\alpha})\sin(\varphi_{\alpha,\beta})\right)\Big]. \end{aligned} \quad (47)$$

Averaging over phase disorder leads to

$$\langle\langle \Lambda^{\rm AF}_{\rm Mixed}\rangle\rangle = 1 - \frac{1}{2}\frac{a_0^2}{R^2_{\alpha,\beta}}\left(\frac{|t_0^{a,\alpha}|^2}{1+|t_0^{a,\alpha}|^2}\right) - \frac{1}{2}\frac{a_0^2}{R^2_{\alpha',\beta}}\left(\frac{|t_0^{a',\alpha'}|^4}{1+|t_0^{a',\alpha'}|^4}\right) + \frac{1}{2}\frac{a_0^3}{R_{\alpha,\beta}R_{\alpha',\beta}R_{\alpha,\alpha'}}\left(\frac{|t_0^{a,\alpha}|^2}{1+|t_0^{a,\alpha}|^2}\right)\left(\frac{|t_0^{a',\alpha'}|^4}{1+|t_0^{a',\alpha'}|^4}\right) \quad (48)$$

$$\langle\langle \Lambda^{\rm F}_{\rm Mixed}\rangle\rangle = 1 - \frac{1}{2}\frac{a_0^2}{R^2_{\alpha,\beta}}\left(\frac{|t_0^{a,\alpha}|^2}{1+|t_0^{a,\alpha}|^2}\right)\sin^2(\varphi_{\alpha,\beta}) + \frac{1}{2}\frac{a_0^2}{R^2_{\alpha',\beta}}\left(\frac{|t_0^{a',\alpha'}|^4}{1+|t_0^{a',\alpha'}|^4}\right) + \frac{a_0^3}{R_{\alpha,\beta}R_{\alpha',\beta}R_{\alpha,\alpha'}}\left(\frac{|t_0^{a,\alpha}|^2}{1+|t_0^{a,\alpha}|^2}\right)\left(\frac{|t_0^{a',\alpha'}|^4}{1+|t_0^{a',\alpha'}|^4}\right). \quad (49)$$

As a consequence this heterostructure behaves like the full metallic heterostructure ($\delta_\beta > 0$).

3.5 Lowest order diagrams

In this section we point out a simple rule that can be used to determine whether $\Delta^{\rm F}_\beta > \Delta^{\rm AF}_\beta$ or whether $\Delta^{\rm F}_\beta < \Delta^{\rm AF}_\beta$. Let us start with the metallic model. We see from equation (22) and equations (25–26) that the lowest order non local process are given by

$$g^{\beta,\alpha}t^{\alpha,a}g^{a,a}_{1,1}t^{a,\alpha}f^{\alpha,\alpha'}t^{\alpha',a'}g^{a',a'}_{2,2}t^{a',\alpha'}g^{\alpha',\beta} \quad (50)$$

if the ferromagnets have an antiparallel spin orientation, and by

$$g^{\beta,\alpha}t^{\alpha,a}g^{a,a}_{1,1}t^{a,\alpha}g^{\alpha,\alpha'}t^{\alpha',a'}g^{a',a'}_{1,1}t^{a',\alpha'}f^{\alpha',\beta} \quad (51)$$

$$f^{\beta,\alpha}t^{\alpha,a}g^{a,a}_{1,1}t^{a,\alpha}g^{\alpha,\alpha'}t^{\alpha',a'}g^{a',a'}_{1,1}t^{a',\alpha'}g^{\alpha',\beta} \quad (52)$$

if the ferromagnets have a parallel spin orientation. The corresponding diagrams are shown in Figure 9. Because

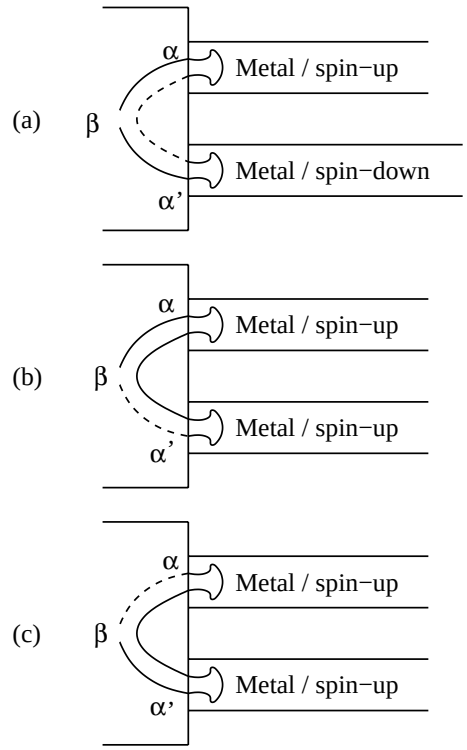

Fig. 9. Lowest order processes in the case of metallic ferromagnets. (a) corresponds to (50), (b) corresponds to (51), and (c) corresponds to (52).

each of these diagrams contains four "g" propagators and one "f" propagator, the sign of the coefficient of the non local term in $\Lambda^{\rm F}_{\rm Metal}$ and $\Lambda^{\rm AF}_{\rm Metal}$ is positive (in agreement with Eqs. (29, 33)). There is one diagram in the case of parallel spin orientations, and there are two diagrams in the case of antiparallel spin orientations, which explains the factor of two appearing in the case of a parallel spin orientation – see equations (29, 33).

Let us now consider insulating ferromagnets. The lowest order diagrams are given by (50, 51) and (52) but now $g^{a,a}$ and $g^{a',a'}$ are real numbers. As a consequence the sign of the non local term with insulating ferromagnets is opposite to the sign of the non local term with metallic ferromagnets, which is in agreement with equations (36, 37).

Finally in the mixed case the diagrams given by (50, 51) and (52) cancel because they are pure imaginary. Therefore we look for the diagrams appearing in the next order. One of these diagrams is represented in Figure 10. There are four "g" propagators involved. The sign of the diagram is positive, which explains why the mixed junction behaves like the metallic junction. The diagram in Figure 10 is proportional to $|t^{a,\alpha}|^2|t^{a',\alpha'}|^4$, which is in agreement with equations (48, 49).

3.6 Ferromagnetic electrodes with both spin channels

In this section we calculate the superconducting gap of a superconductor connected to one-dimensional ferromagnetic electrodes having a partial spin polarization. The motivation is to show that the results obtained in the preceding section for half-metal ferromagnets are valid also in the presence of a partial spin polarization. The ferromagnetic electrodes are described by the Stoner Hamiltonian (2) in which the exchange field is smaller than the Fermi energy. The spin-up and spin-down channels are characterized by the density of states $\rho_\uparrow$ and $\rho_\downarrow$ (see Eqs. (5, 6)). The derivations of the results is given in Appendix B.

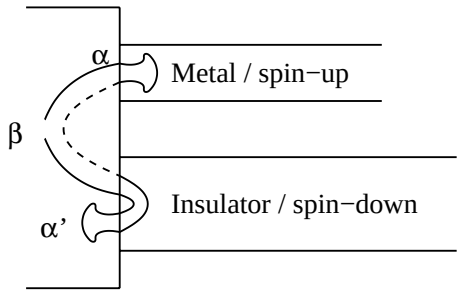

Fig. 10. Lowest order processes in the case of the mixed junction with antiparallel spin orientations.

We use equations (B.4–B.7) and equations (B.8–B.11) obtained in Appendix B and the local approximation already discussed in Section 3. We find that the high energy behavior of the Gorkov function is given by (28) and (30), with the following parameters $\Lambda^{\rm Ferro}_{\rm Metal}$ and $\Lambda^{\rm AF}_{\rm Metal}$:

$$\langle\langle \Lambda^{\rm AF}_{\rm Metal}\rangle\rangle = 1 - \frac{1}{2}\frac{a_0^2}{R^2_{\alpha,\beta}}\frac{x_\uparrow + x_\downarrow}{(1+x_\uparrow)(1+x_\downarrow)} - \frac{1}{2}\frac{a_0^2}{R^2_{\alpha',\beta}}\frac{x_\uparrow + x_\downarrow}{(1+x_\uparrow)(1+x_\downarrow)} - \frac{1}{2}\frac{a_0^3}{R_{\alpha,\beta}R_{\alpha',\beta}R_{\alpha,\alpha'}} \times \frac{x_\uparrow^2 + x_\downarrow^2 + 2x_\uparrow^2 x_\downarrow + 2x_\uparrow x_\downarrow^2 + 4x_\uparrow x_\downarrow - 2x_\uparrow^2 x_\downarrow^2}{(1+x_\uparrow)^2(1+x_\downarrow)^2} \quad (53)$$

$$\langle\langle \Lambda^{\rm Ferro}_{\rm Metal}\rangle\rangle = 1 - \frac{1}{2}\frac{a_0^2}{R^2_{\alpha,\beta}}\frac{x_\uparrow + x_\downarrow}{(1+x_\uparrow)(1+x_\downarrow)} - \frac{1}{2}\frac{a_0^2}{R^2_{\alpha',\beta}}\frac{x_\uparrow + x_\downarrow}{(1+x_\uparrow)(1+x_\downarrow)} - \frac{a_0^3}{R_{\alpha,\beta}R_{\alpha',\beta}R_{\alpha,\alpha'}} \times \frac{x_\uparrow^2 + x_\downarrow^2 + x_\uparrow^2 x_\downarrow + x_\uparrow x_\downarrow^2 + x_\uparrow x_\downarrow - x_\uparrow^2 x_\downarrow^2}{(1+x_\uparrow)^2(1+x_\downarrow)^2}, \quad (54)$$

where $x_\uparrow$ and $x_\downarrow$ are given by equations (7, 8). The case of half-metal ferromagnets discussed in Section 3 can be recovered by considering the limit $x_\downarrow = 0$, in which case equations (53, 54) reduce to equations (42, 43). On the other hand it is easy to show from equations (53, 54) that the ferromagnetic and antiferromagnetic superconducting gaps are equal only if there is no spin polarization ($\rho_\uparrow = \rho_\downarrow$). As a consequence for two metallic ferromagnets having an arbitrary small spin polarization, the ferromagnetic gap is larger than the antiferromagnetic gap. This

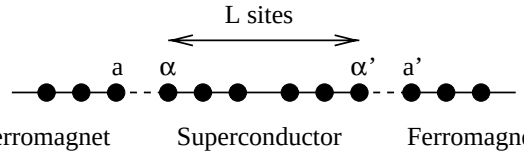

Fig. 11. The geometry treated in the numerical simulation. A superconductor on a one dimensional segment with L sites is connected to two ferromagnets.

generalizes the behavior obtained in Section 3 in the case of half-metal ferromagnets.

4 Exact diagonalizations for half-metal ferromagnets

We present in this section a simulation based on exact diagonalizations in which we can iterate the functional form of the self consistency equation given by equation (12). The method is presented in Sections 4.1 and 4.2. The results are discussed in Section 4.3.

4.1 Bogoliubov-de Gennes equations

4.1.1 Bogoliubov-de Gennes Hamiltonian

We consider the BCS model defined by equation (1) on a one dimensional lattice with L sites (see Fig. 11):

$$\hat{\mathcal{H}} - \mu\hat{N} = \sum_{\sigma,i=1}^{L} -t\left(c^{+}_{i+1,\sigma}c_{i,\sigma} + c^{+}_{i,\sigma}c_{i+1,\sigma}\right) + \sum_{i=1}^{L}\Delta_i\left(c^{+}_{i,\uparrow}c^{+}_{i,\downarrow} + c_{i,\downarrow}c_{i,\uparrow}\right) - \mu\hat{N}. \quad (55)$$

The two dimensional model cannot be treated numerically because of computational limitations and this is why we consider a one dimensional geometry. Nevertheless, the method that we use in 1D can be also applied to 2D models. It is convenient to use the notation

$$\check{\psi}^{+}_{\uparrow} = \left[c^{+}_{1,\uparrow}, ..., c^{+}_{L,\uparrow}, c_{1,\downarrow}, ..., c_{L,\downarrow}\right], \quad (56)$$

in which $\check{\psi}^{+}_{\uparrow}$ has $2L$ components. We use (56) to obtain the Bogoliubov-de Gennes Hamiltonian

$$\check{H} = \check{\psi}^{+}_{\uparrow}\check{K}\check{\psi}_{\uparrow} + \check{\psi}^{+}_{\uparrow}\check{\Delta}\check{\psi}_{\uparrow}, \quad (57)$$

where the kinetic term is

$$\check{K}^{1,1}_{i,j} = -t\left(\delta_{i,j+1} + \delta_{i,j-1}\right) + \mu\delta_{i,j} \quad (58)$$

$$\check{K}^{2,2}_{k,l} = t\left(\delta_{k,l+1} + \delta_{k,l-1}\right) - \mu\delta_{k,l} \quad (59)$$

$$\check{K}^{1,2}_{i,k} = \check{K}^{2,1}_{k,i} = 0, \quad (60)$$

and the pairing term is

$$\check{\Delta}^{1,1}_{i,j} = \check{\Delta}^{2,2}_{i,j} = 0 \quad (61)$$

$$\check{\Delta}^{1,2}_{i,k} = \check{\Delta}^{2,1}_{k,i} = \Delta_i\delta_{i,k}. \quad (62)$$

Similarly to the Nambu representation, we have used the label "1" for the "electronic" components of $\check{\psi}$ and the label "2" for the"hole" components. We have doubled the space coordinates: the labels i, j correspond to the electronic component and the labels k, l correspond to the hole component. The symbol $\delta_{i,k}$ means that i and k correspond to the same site on the lattice but belong to a different Nambu component.

4.1.2 Spectral representations

The eigenvectors of the Bogoliubov-de Gennes Hamiltonian (57) take the form

$$|\psi_\alpha\rangle = \sum_{i=1}^{L} R_{\alpha,i}|e_i\rangle + \sum_{k=1}^{L} R_{\alpha,k}|e_k\rangle \quad (63)$$

$$|\psi_\beta\rangle = \sum_{i=1}^{L} R_{\beta,i}|e_i\rangle + \sum_{k=1}^{L} R_{\beta,k}|e_k\rangle, \quad (64)$$

where the eigenvalues are such that $\lambda_\alpha > 0$ and $\lambda_\beta < 0$. In this notation there are L kets $|e_i\rangle$ associated to the first component of the Nambu representation, and there are L kets $|e_k\rangle$ associated to the second component of the Nambu representation. We deduce from equations (63, 64) the form of the quasiparticle operators

$$\Gamma^{+}_{\alpha,\downarrow} = \sum_i R_{\alpha,i}c_{i,\uparrow} + \sum_k R_{\alpha,k}c^{+}_{k,\downarrow} \quad (65)$$

$$\Gamma_{\beta,\uparrow} = \sum_i R_{\beta,i}c_{i,\uparrow} + \sum_k R_{\beta,k}c^{+}_{k,\downarrow} \quad (66)$$

which diagonalize the Bogoliubov-de Gennes Hamiltonian

$$\hat{\mathcal{H}} = \sum_\alpha \lambda_\alpha\Gamma^{+}_{\alpha,\downarrow}\Gamma_{\alpha,\downarrow} - \sum_\beta \lambda_\beta\Gamma^{+}_{\beta,\uparrow}\Gamma_{\beta,\uparrow}.$$

The spectral representation of the Green's function (10) can be expressed in terms of the matrix R:

$$g^{A,1,1}_{i,j} = \sum_\beta \frac{R_{\beta,i}R_{\beta,j}}{\omega + i\eta - [\mu + |E_\beta|]} + \sum_\alpha \frac{R_{\alpha,i}R_{\alpha,j}}{\omega + i\eta - [\mu - E_\alpha]} \quad (67)$$

$$g^{A,1,2}_{i,k} = \sum_\beta \frac{R_{\beta,i}R_{\beta,k}}{\omega + i\eta - [\mu + |E_\beta|]} + \sum_\alpha \frac{R_{\alpha,i}R_{\alpha,k}}{\omega + i\eta - [\mu - E_\alpha]}\,. \quad (68)$$

4.2 Evaluation of the Green's functions

4.2.1 Evaluation of a spectral representation:

The Green's functions are obtained from equations (67, 68) in terms of their poles ω_n and residues R_n:

$$g_0^A(\omega) = \sum_n \frac{R_n}{\omega - \omega_n - \mathrm{i}\eta} \cdot \tag{69}$$

To make the integration over energy, we go to the limit of zero dissipation ($\eta \to 0$) and use the identity $1/[\omega - \omega_n - \mathrm{i}\eta] = \mathcal{P}/[\omega - \omega_n] + \mathrm{i}\pi\delta(\omega - \omega_n)$. To show that the principal part can be neglected if $\omega > \Delta$, we come back to the particular case where the superconducting order parameter is uniform: $\Delta_\beta \equiv \Delta_0$ for all β. In this case the spectral representation takes the form

$$g^A_{\alpha,\beta}(\omega) = \frac{1}{\mathcal{N}} \sum_{\mathbf{k}} \mathrm{e}^{\mathrm{i}\mathbf{k}.(\mathbf{x}_\alpha - \mathbf{x}_\beta)} \times \left[\frac{|u_k|^2}{\omega - (\mu_S + E_k) - \mathrm{i}\eta} + \frac{|v_k|^2}{\omega - (\mu_S - E_k) - \mathrm{i}\eta} \right] \cdot \tag{70}$$

We start from equation (70) and make the substitution

$$\frac{1}{\omega - (\mu_S + E_k) - \mathrm{i}\eta} \to \mathrm{i}\pi\delta\left(\omega - (\mu_S + E_k)\right) \tag{71}$$

$$\frac{1}{\omega - (\mu_S - E_k) - \mathrm{i}\eta} \to \mathrm{i}\pi\delta\left(\omega - (\mu_S - E_k)\right) \cdot \tag{72}$$

The Green's function given by equation (70) becomes

$$g^A_{\alpha,\beta} \to \mathrm{i}\pi \frac{1}{\mathcal{N}} \sum_{\mathbf{k}} \mathrm{e}^{\mathrm{i}\mathbf{k}.(\mathbf{x}_\alpha - \mathbf{x}_\beta)} \times \left[(u_k)^2 \delta\left(\omega - (\mu_S + E_k)\right) + (v_k)^2 \delta\left(\omega - (\mu_S - E_k)\right) \right] \cdot \tag{73}$$

After using the δ-function (73) and performing the integral over wave vector we recover the form (16) of the Green's function in which the term proportional to $\cos\varphi$ has been discarded. The fact that the term proportional to $\cos\varphi$ is not included does not constitute a problem because we know from Section 3 that the envelope of the $2k_\mathrm{F}$-oscillations is the same in the presence or absence of the $\cos\varphi$ term. Therefore if $\omega > \Delta$, equation (69) can be replaced by

$$g_0^A(\omega) = \mathrm{i}\pi \sum_n R_n \delta\left(\omega - \omega_n\right) \cdot \tag{74}$$

4.2.2 Evaluation of the δ-functions

To evaluate the δ-function in (74), we replace $\delta(\omega - \omega_n)$ by $\delta_\eta(\omega)$, where $\delta_\eta(\omega)$ is a function having a width η in energy, and normalized to unity: $\int \delta_\eta(\omega)\mathrm{d}\omega = 1$. For instance $\delta_\eta(\omega)$ can be chosen as a Lorentzian or a Gaussian. To obtain the value of a Green's function at a single energy ω the Lorentzian or Gaussian will be evaluated $2L$ times. To optimize this part of the program, it is useful to use a function $\delta_\eta(\omega)$ that is finite only in the interval $[-\eta, \eta]$ and vanishes outside this energy interval. The simplest choice is given by

$$\delta_\eta(\omega) = \frac{3}{4\eta}\left[1 - \left(\frac{\omega}{\eta}\right)^2\right] \text{ if } |\omega| < \eta. \tag{75}$$

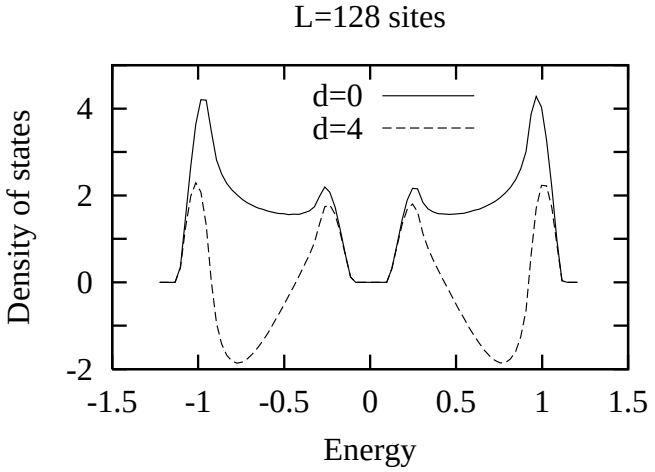

Fig. 12. Energy dependence of the density of state $\rho_g^{\alpha,\beta}$, for two values of the distance between the sites α and β. We used periodic boundary conditions, with $L = 128$ sites. The hopping energy is $t = 0.5$, the superconducting gap $\Delta_0 = 0.2$ is uniform and the level broadening is $\eta = 0.1$.

4.3 Results

We consider the geometry represented in Figure 11 in which a one dimensional superconductor on an open segment with L sites is connected to two ferromagnetic metals. The superconductor is described by the BCS tight-binding Hamiltonian (1). We note $t_0 = t_{a,\alpha}/t = t_{a',\alpha'}/t$ the tunnel matrix element connecting the ferromagnets and the superconductor, normalized to the bandwidth of the superconductor. Low transparency interfaces correspond to $t_0 \ll 1$ and high transparency interfaces correspond to $t_0 \sim 1$.

4.3.1 Density of states

We have shown in Figure 12 the energy dependence of the density of states $\rho_g^{\alpha,\beta}$ associated to the ordinary propagator (see Sect. 2.2) in the presence of a uniform gap profile $\Delta_\beta \equiv \Delta_0$ for all β, and with $L = 128$ sites. It is visible in this figure that the different parameters of the simulation are compatible with each other. Namely, the level broadening η is sufficiently small to have a well-defined superconducting gap. The level broadening is also sufficiently large for quasiparticle states to form a continuous

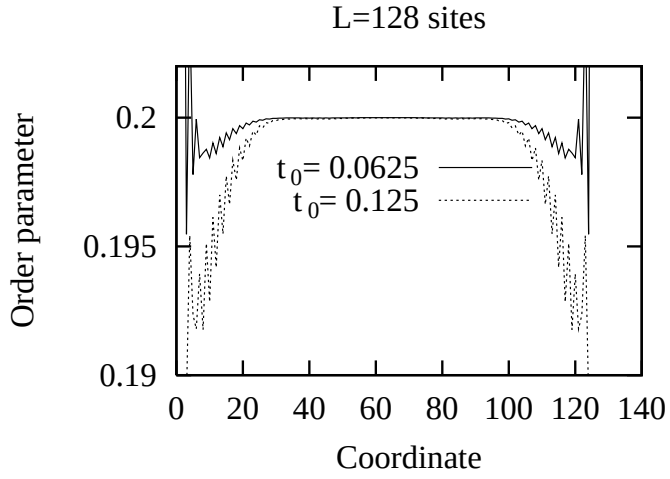

Fig. 13. Self consistent gap profile with $L = 128$ sites and two values of t_0: $t_0 = 0.0625$ (solid line) and $t_0 = 0.125$ (dotted line). The other parameters are the same as in Figure 12. The difference between the parallel and the antiparallel superconducting order parameters cannot be distinguished on the scale of the figure.

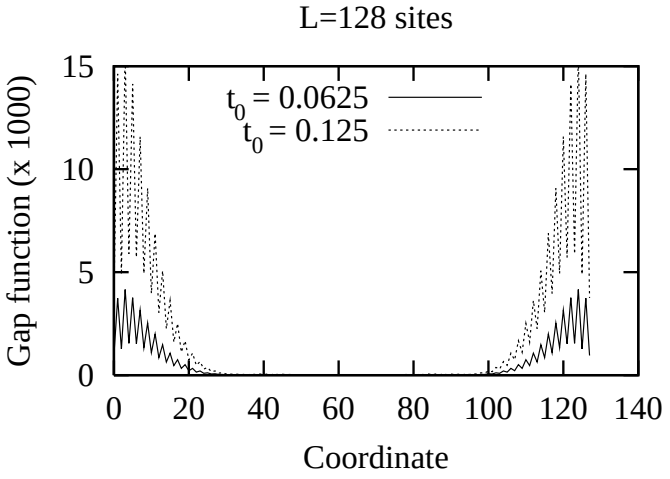

Fig. 14. Variation of δ_β defined by (34) with $L = 128$ sites in the superconductor. The parameters are identical to Figure 13.

band. Because of these two constraints, we cannot use in this simulation realistic parameters as we did for the local approach in Section 3 (see Fig. 3). Using realistic parameters would require too large system sizes.

Finally, the calculation of the superconducting order parameter presented in Section 3 were based on the estimation of the Gorkov function at high energy. By contrast low energy degrees of freedom play a relevant role in our simulation. One of the questions that will be answered by the exact diagonalizations is to determine whether low energy degrees of freedom (probed by the numerical simulation with strong finite size effects) have the same physics as high energy degrees of freedom (probed by the local approach in Sect. 3).

4.3.2 Gap profile

The gap profile is shown in Figure 13 for $L = 128$ sites. We have obtained similar results for $L = 32$ and $L = 64$ sites. The gap profile obtained with exact diagonalizations is qualitatively similar to Section 3. Namely, the superconducting order parameter is reduced close to the interface with the ferromagnets and we obtain $2k_\mathrm{F}$ oscillations in the gap profile.

4.3.3 Difference between the superconducting gaps in the ferromagnetic and antiferromagnetic alignments

We have shown in Figure 14 the variation of δ_β defined by equation (34) with $L = 128$ sites. Similar results have been obtained with $L = 32$ and $L = 64$ sites. For each site β in the superconductor, we have calculated the superconducting order parameters Δ_β^F and $\Delta_\beta^{\mathrm{AF}}$ with parallel and antiparallel spin orientations in the two ferromagnetic electrodes. From what we deduce the value of δ_β defined by equation (34). The calculation consists in iterating the process in Figure 1 until a sufficient precision has been obtained. The relative error made in the determination of the order parameters is several orders of magnitude smaller than the difference between the ferromagnetic and antiferromagnetic superconducting gaps.

We made the simulations with two values of the normalized hopping between the superconductor and the ferromagnet (see Fig. 14). We also tried larger values of the interface transparencies but the algorithm did not converge. The clarification of this point is left as an open question for future work. From the result presented in Figure 14 we deduce that

(i) With all available sizes and interface transparencies, δ_β defined by (34) is positive, meaning that *the gap is larger in the ferromagnetic alignment*. This is opposite to the model with insulating ferromagnets [42] and is in agreement with the approaches used in Sections 3 and 3.6.

(ii) δ_β defined by equation (34) tends to zero in the bulk of the superconductor. The cross-over between the surface and bulk behavior is controlled by a length scale which is of order 10 in Figure 14. It is expected that this length scale is equal to the superconducting coherence length given by $\xi_0 = \epsilon_\mathrm{F}/(k_\mathrm{F}\Delta_0)$.

5 Conclusion

To summarize, we have provided a detailed investigation of F/S/F trilayers with metallic ferromagnets. We found that the physics of the metallic trilayer was dominated by pair correlations, not by pair breaking. This behavior was obtained with several complementary approaches:

(i) An approach based on the estimation of the high energy behavior of the Gorkov function for half-metal

ferromagnets (see Sect. 3) and for ferromagnets having both spin conduction channels (see Sect. 3.6). In these approaches we could use realistic parameters ($\Delta_{\rm bulk}/D = 10^{-4}$).

(ii) *Exact diagonalizations* (see Sect. 4) that were limited to small sizes and large values of $\Delta_{\rm bulk}/D$ ($\Delta_{\rm bulk}/D = 0.2$).

In all approaches we find that the F/S/F trilayer with metallic ferromagnets is characterized by $\Delta_{\rm F} > \Delta_{\rm AF}$ while the F/S/F trilayer with insulating ferromagnets is characterized by $\Delta_{\rm AF} > \Delta_{\rm F}$.

Finally, we mention two recent theoretical articles [39] in which Usadel equations have been used to treat F/S/F heterostructures in the diffusive regime. These authors have found that the metallic F/S/F heterostructure was controlled by pair breaking ($\Delta_{\rm F} < \Delta_{\rm AF}$) while we have found here an opposite behavior ($\Delta_{\rm F} > \Delta_{\rm AF}$). In fact we believe that both approaches are correct but do not incorporate the same ingredients. The behavior of the model that we consider here is strongly related to non local pair correlations and can be explained with lowest order diagrams. The existence of a simple explanation shows the validity of the picture proposed in our article. On the other hand the model considered in reference [39] is well suited to describe diffusive heterostructures. We are not certain at the present stage that the usual form of Usadel equations can be used to describe non local processes as we did here in ballistic systems. We think that a lot of understanding can be gained by discussing non local Usadel equations.

The authors acknowledge fruitful discussions with A. Buzdin, J.C. Cuevas and D. Feinberg.

Appendix A: Expression of the Keldysh propagators

The goal of this appendix is to rederive the main results of this article with the non equilibrium form (11) of the Gorkov function, rather than the equilibrium Gorkov function (13). This formalism based on non equilibrium Green's functions is more general than the equilibrium Green's function formalism because it can also be applied to non equilibrium problems. A detailed investigation of this issue will be presented in the future. Here, we want to show that both formalisms coincide for the equilibrium problem, which constitutes also a test of the calculations presented in the main body of the article.

A.1 One-channel problem

Let us first consider the single channel model (see Fig. 2). The Green's functions $G^{R,A}$ are the solution of the Dyson equation

$$\hat{G}^{a,a} = \hat{g}^{a,a} + \hat{g}^{a,a}\hat{t}^{a,\alpha}\hat{g}^{\alpha,\alpha}\hat{t}^{\alpha,a}\hat{G}^{a,a},$$

from what we deduce $G^{a,a}_{1,1} = g^{a,a}_{1,1}/\mathcal{D}$, with $\mathcal{D}$ given by (19). The Dyson-Keldysh equation associated to an arbitrary site in the superconductor takes the form

$$\begin{aligned}\hat{G}^{+,-}_{\beta,\beta} &= \hat{g}^{+,-}_{\beta,\beta} + \hat{g}^{+,-}_{\beta,\alpha}\hat{t}_{\alpha,a}\hat{G}^{A}_{a,\beta} + \hat{G}^{R}_{\beta,a}\hat{t}_{\alpha,a}\hat{g}^{+,-}_{\alpha,\beta}\\ &+ \hat{G}^{R}_{\beta,a}\hat{t}_{a,\alpha}\hat{g}^{+,-}_{\alpha,\alpha}\hat{t}_{\alpha,a}\hat{G}^{A}_{a,\beta} + \hat{G}^{R}_{\beta,\alpha}\hat{t}_{\alpha,a}\hat{g}^{+,-}_{a,a}\hat{t}_{a,\alpha}\hat{G}^{A}_{\alpha,\beta}. \quad \text{(A.1)}\end{aligned}$$

Evaluating the five terms in (A.1) leads to

$$\begin{aligned}G^{+,-}_{\beta,\beta} = 2{\rm i}\pi n_{\rm F}(\omega-\mu_S)\Big\{&\rho^{\beta,\beta}_f + |t_{a,\alpha}|^2\frac{1}{\mathcal{D}^A}g^{a,a,A}_{1,1}f^{\alpha,\beta,A}\rho^{\beta,\alpha}_g\\ &+|t_{a,\alpha}|^2\frac{1}{\mathcal{D}^R}g^{a,a,R}_{1,1}g^{\beta,\alpha,R}\rho^{\alpha,\beta}_f\\ &+ |t^{a,\alpha}|^4\frac{1}{\mathcal{D}^A\mathcal{D}^R}g^{a,a,A}_{1,1}g^{a,a,R}_{1,1}g^{\beta,\alpha,R}f^{\alpha,\beta,A}\rho^{\alpha,\alpha}_g\Big\}\\ &+ 2{\rm i}\pi n_{\rm F}(\omega-\mu_a)|t^{a,\alpha}|^2\frac{1}{\mathcal{D}^A\mathcal{D}^R}g^{\beta,\alpha,R}f^{\alpha,\beta,A}\rho^{a,a}_{1,1}. \quad \text{(A.2)}\end{aligned}$$

The final step is to show that with $\mu_a = \mu_S$ this expression coincides with (18).

A.2 Two-channel problem with antiparallel magnetizations

The Dyson-Keldysh equation associated to an arbitrary site β in the superconductor is the following:

$$\begin{aligned}\hat{G}^{+,-}_{\beta,\beta} &= \hat{g}^{+,-}_{\beta,\beta} + \hat{g}^{+,-}_{\beta,\alpha}\hat{t}_{\alpha,a}\hat{G}^{A}_{a,\beta} + \hat{g}^{+,-}_{\beta,\alpha'}\hat{t}_{\alpha',a'}\hat{G}^{A}_{a',\beta}\\ &+ \hat{G}^{R}_{\beta,a}\hat{t}_{a,\alpha}\hat{g}^{+,-}_{\alpha,\beta} + \hat{G}^{R}_{\beta,a'}\hat{t}_{a',\alpha'}\hat{g}^{+,-}_{\alpha',\beta} + \hat{G}^{R}_{\beta,a}\hat{t}_{a,\alpha}\hat{g}^{+,-}_{\alpha,\alpha}\hat{t}_{\alpha,a}\hat{G}^{A}_{a,\beta}\\ &+ \hat{G}^{R}_{\beta,a'}\hat{t}_{a',\alpha'}\hat{g}^{+,-}_{\alpha',\alpha'}\hat{t}_{\alpha',a'}\hat{G}^{A}_{a',\beta} + \hat{G}^{R}_{\beta,a}\hat{t}_{a,\alpha}\hat{g}^{+,-}_{\alpha,\alpha'}\hat{t}_{\alpha',a'}\hat{G}^{A}_{a',\beta}\\ &+ \hat{G}^{R}_{\beta,a'}\hat{t}_{a',\alpha'}\hat{g}^{+,-}_{\alpha',\alpha}\hat{t}_{\alpha,a}\hat{G}^{A}_{a,\beta} + \hat{G}^{R}_{\beta,\alpha}\hat{t}_{\alpha,a}\hat{g}^{+,-}_{a,a}\hat{t}_{a,\alpha}\hat{G}^{A}_{\alpha,\beta}\\ &+ \hat{G}^{R}_{\beta,\alpha'}\hat{t}_{\alpha',a'}\hat{g}^{+,-}_{a',a'}\hat{t}_{a',\alpha'}\hat{G}^{A}_{\alpha',\beta}. \quad \text{(A.3)}\end{aligned}$$

We need the expression of the following Green's functions:

$$\hat{G}^{\beta,a} = t^{a,\alpha}g^{a,a}_{1,1}\begin{bmatrix}\tilde{g}^{\beta,\alpha} & 0\\ \tilde{f}^{\beta.\alpha} & 0\end{bmatrix} \quad \text{(A.4)}$$

$$\hat{G}^{\beta,a'} = -t^{a',\alpha'}g^{a',a'}_{2,2}\begin{bmatrix}0 & \tilde{f}^{\beta,\alpha'}\\ 0 & \tilde{g}^{\beta,\alpha'}\end{bmatrix} \quad \text{(A.5)}$$

$$\hat{G}^{\alpha,\beta} = \begin{bmatrix}\tilde{g}^{\alpha,\beta} & \tilde{f}^{\alpha,\beta}\\ G^{\alpha,\beta}_{2,1} & G^{\alpha,\beta}_{2,2}\end{bmatrix} \quad \text{(A.6)}$$

$$\hat{G}^{\beta,\alpha} = \begin{bmatrix}\tilde{g}^{\beta,\alpha} & \tilde{G}^{\beta,\alpha}_{1,2}\\ \tilde{f}^{\beta,\alpha} & G^{\beta,\alpha}_{2,2}\end{bmatrix} \quad \text{(A.7)}$$

$$\hat{G}^{\alpha',\beta} = \begin{bmatrix}G^{\alpha',\beta}_{1,1} & G^{\alpha',\beta}_{1,2}\\ \tilde{f}^{\alpha',\beta} & \tilde{g}^{\alpha',\beta}\end{bmatrix} \quad \text{(A.8)}$$

$$\hat{G}^{\beta,\alpha'} = \begin{bmatrix}G^{\beta,\alpha'}_{1,1} & \tilde{f}^{\beta,\alpha'}\\ G^{\beta,\alpha'}_{2,1} & \tilde{g}^{\beta,\alpha'}\end{bmatrix}. \quad \text{(A.9)}$$

We deduce from (23–26) and (A.4–A.9) the final form of the Gorkov function in the antiparallel alignment:

See equation (A.10) next page.

Using the propagators obtained in Section 3.2.1 to evaluate (A.10), we can show that equation (A.10) leads directly to (28) and (29).

$$\hat{G}^{+,-}_{\beta,\beta} = 2\mathrm{i}\pi n_{\mathrm{F}}(\omega-\mu_S)\Big\{\rho_f^{\beta,\beta} + |t^{a,\alpha}|^2 g_{1,1}^{a,a,A}\tilde{f}^{\alpha,\beta,A}\rho_g^{\beta,\alpha} + |t^{a',\alpha'}|^2 g_{2,2}^{a',a',A}\tilde{g}^{\alpha',\beta,A}\rho_f^{\beta,\alpha'} + |t^{a,\alpha}|^2 g_{1,1}^{a,a,R}\tilde{g}^{\beta,\alpha,R}\rho_f^{\alpha,\beta}$$
$$+|t^{a',\alpha'}|^2 g_{2,2}^{a',a',R}\tilde{f}^{\beta,\alpha',R}\rho_g^{\alpha',\beta} + |t^{a,\alpha}|^4 g_{1,1}^{a,a,R}g_{1,1}^{a,a,A}\tilde{g}^{\beta,\alpha,R}\tilde{f}^{\alpha,\beta,A}\rho_g^{\alpha,\alpha} + |t^{a',\alpha'}|^4 g_{2,2}^{a',a',R}g_{2,2}^{a',a',A}\tilde{g}^{\alpha',\beta,A}\tilde{f}^{\beta,\alpha',R}\rho_g^{\alpha',\alpha'}$$
$$+ |t^{a,\alpha}|^2|t^{a',\alpha'}|^2 g_{1,1}^{a,a,R}g_{2,2}^{a',a',A}\tilde{g}^{\beta,\alpha,R}\tilde{g}^{\alpha',\beta,A}\rho_f^{\alpha,\alpha'} + |t^{a,\alpha}|^2|t^{a',\alpha'}|^2 g_{1,1}^{a,a,A}g_{2,2}^{a',a',R}\tilde{f}^{\beta,\alpha',R}\tilde{f}^{\alpha,\beta,A}\rho_f^{\alpha',\alpha}\Big\}$$
$$+2\mathrm{i}\pi n_{\mathrm{F}}(\omega-\mu_a)|t^{a,\alpha}|^2\tilde{g}^{\beta,\alpha,R}\tilde{f}^{\alpha,\beta,A}\rho_{1,1}^{a,a} + 2\mathrm{i}\pi n_{\mathrm{F}}(\omega-\mu_{a'})|t^{a',\alpha'}|^2\tilde{f}^{\beta,\alpha',R}\tilde{g}^{\alpha',\beta,A}\rho_{2,2}^{a',a'}. \quad (A.10)$$

$$\hat{G}^{+,-}_{\beta,\beta} = 2\mathrm{i}\pi n_{\mathrm{F}}(\omega-\mu_S)\Big\{\rho_f^{\beta,\beta} + |t^{a,\alpha}|^2 g_{1,1}^{a,a,A}\tilde{f}^{\alpha,\beta,A}\rho_g^{\beta,\alpha} + |t^{a',\alpha'}|^2 g_{1,1}^{a',a',A}\tilde{f}^{\alpha',\beta,A}\rho_g^{\beta,\alpha'} + |t^{a,\alpha}|^2 g_{1,1}^{a,a,R}\tilde{g}^{\beta,\alpha,R}\rho_f^{\alpha,\beta}$$
$$+|t^{a',\alpha'}|^2 g_{1,1}^{a',a',R}\tilde{g}^{\beta,\alpha',R}\rho_f^{\alpha',\beta} + |t^{a,\alpha}|^4 g_{1,1}^{a,a,R}g_{1,1}^{a,a,A}\tilde{g}^{\beta,\alpha,R}\tilde{f}^{\alpha,\beta,A}\rho_g^{\alpha,\alpha} + |t^{a',\alpha'}|^4 g_{1,1}^{a',a',R}g_{1,1}^{a',a',A}\tilde{f}^{\alpha',\beta,A}\tilde{g}^{\beta,\alpha',R}\rho_g^{\alpha',\alpha'}$$
$$+ |t^{a,\alpha}|^2|t^{a',\alpha'}|^2 g_{1,1}^{a,a,R}g_{1,1}^{a',a',A}\tilde{g}^{\beta,\alpha,R}\tilde{f}^{\alpha',\beta,A}\rho_g^{\alpha',\alpha} + |t^{a,\alpha}|^2|t^{a',\alpha'}|^2 g_{1,1}^{a,a,A}g_{1,1}^{a',a',R}\tilde{g}^{\beta,\alpha',R}\tilde{f}^{\alpha,\beta,A}\rho_g^{\alpha',\alpha}\Big\}$$
$$+2\mathrm{i}\pi n_{\mathrm{F}}(\omega-\mu_a)|t^{a,\alpha}|^2\tilde{g}^{\beta,\alpha,R}\tilde{f}^{\alpha,\beta,A}\rho_{1,1}^{a,a} + 2\mathrm{i}\pi n_{\mathrm{F}}(\omega-\mu_{a'})|t^{a',\alpha'}|^2\tilde{g}^{\beta,\alpha',R}\tilde{f}^{\alpha',\beta,A}\rho_{1,1}^{a',a'}, \quad (A.11)$$

A.3 Two-channel problem with parallel magnetizations

Let us now consider two single-channel ferromagnetic electrodes having a parallel spin orientation. Following Section A.2, we obtain

See equation (A.11) above

where the propagators $\tilde{g}$ and $\tilde{f}$ are given by

$$\tilde{g}^{\alpha,\beta} = \frac{1}{\mathcal{D}_{\mathrm{F}}}\Big[g^{\alpha,\beta} + |t^{a',\alpha'}|^2 g_{2,2}^{a',a'}\Big(g^{\alpha,\alpha'}g^{\alpha'\beta} - g^{\alpha',\alpha'}g^{\alpha,\beta}\Big)\Big] \quad (A.12)$$

$$\tilde{f}^{\alpha,\beta} = \frac{1}{\mathcal{D}_{\mathrm{F}}}\Big[f^{\alpha,\beta} + |t^{a',\alpha'}|^2 g_{2,2}^{a',a'}\Big(g^{\alpha,\alpha'}f^{\alpha',\beta} - g^{\alpha',\alpha'}f^{\alpha,\beta}\Big)\Big] \quad (A.13)$$

$$\tilde{g}^{\beta,\alpha} = \frac{1}{\mathcal{D}_{\mathrm{F}}}\Big[g^{\beta,\alpha} + |t^{a',\alpha'}|^2 g_{2,2}^{a',a'}\Big(g^{\alpha',\alpha}g^{\beta,\alpha'} - g^{\alpha',\alpha'}g^{\beta,\alpha}\Big)\Big] \quad (A.14)$$

$$\tilde{f}^{\beta,\alpha} = \frac{1}{\mathcal{D}_{\mathrm{F}}}\Big[f^{\beta,\alpha} + |t^{a',\alpha'}|^2 g_{2,2}^{a',a'}\Big(g^{\alpha',\alpha}f^{\beta,\alpha'} - g^{\alpha',\alpha'}f^{\beta,\alpha}\Big)\Big], \quad (A.15)$$

where $\mathcal{D}_{\mathrm{F}}$ is given by equation (32). We can show that equation (A.11) leads directly to (30) and (33).

Appendix B: Ferromagnetic electrodes with an arbitrary spin polarization

B.1 Dyson matrix

The advanced and retarded Green's function $\hat{G}_{\beta,\beta}$ at an arbitrary site β of the superconductor can be deduced from equation (9):

$$G_{2,1}^{\beta,\beta} = g_{2,1}^{\beta,\beta} + g_{2,1}^{\beta,\alpha}t^{\alpha,a}G_{1,1}^{a,\beta} - g_{2,2}^{\beta,\alpha}t^{\alpha,a}G_{2,1}^{a,\beta} + g_{2,1}^{\beta,\alpha'}t^{\alpha',a'}G_{1,1}^{a',\beta} - g_{2,2}^{\beta,\alpha'}t^{\alpha',a'}G_{2,1}^{a',\beta}. \quad (B.1)$$

Equation (B.1) can be used to evaluate the equilibrium Gorkov function given by equation (13) and deduce the value of the self-consistent superconducting order parameter. The Green's functions $G_{1,1}^{a,\beta}$, $G_{2,1}^{a,\beta}$, $G_{1,1}^{a',\beta}$ and $G_{2,1}^{a',\beta}$ are the solution of the Dyson equation (9) which can be expressed as a 4×4 Dyson matrix:

$$\begin{bmatrix} 1-K_{1,1}^{a,\alpha}t^{\alpha,a} & K_{1,2}^{a,\alpha}t^{\alpha,a} & -K_{1,1}^{a,\beta}t^{\beta,b} & K_{1,2}^{a,\beta}t^{\beta,b} \\ K_{2,1}^{a,\alpha}t^{\alpha,a} & 1-K_{2,2}^{a,\alpha}t^{\alpha,a} & K_{2,1}^{a,\beta}t^{\beta,b} & -K_{2,2}^{a,\beta}t^{\beta,b} \\ -K_{1,1}^{b,\alpha}t^{\alpha,a} & K_{1,2}^{b,\alpha}t^{\alpha,a} & 1-K_{1,1}^{b,\beta}t^{\beta,b} & K_{1,2}^{b,\beta}t^{\beta,b} \\ K_{2,1}^{b,\alpha}t^{\alpha,a} & -K_{2,2}^{b,\alpha}t^{\alpha,a} & K_{2,1}^{b,\beta}t^{\beta,b} & 1-K_{2,2}^{b,\beta}t^{\beta,b} \end{bmatrix} \times \begin{bmatrix} G_{1,1}^{a,\beta} \\ G_{2,1}^{a,\beta} \\ G_{1,1}^{b,\beta} \\ G_{2,1}^{b,\beta} \end{bmatrix} = \begin{bmatrix} K_{1,1}^{a,\beta} \\ -K_{2,1}^{a,\beta} \\ K_{1,1}^{b,\beta} \\ -K_{2,1}^{b,\beta} \end{bmatrix}. \quad (B.2)$$

The coefficients $K_{i,j}$ are of the form $K_{i,j} = g_{i,i}tg_{i,j}$. For instance, $K_{i,j}^{a,\alpha} = g_{i,i}^{a,a}t^{a,\alpha}g_{i,j}^{\alpha,\alpha}$. The inversion of equation (B.2) is described in Section B.2 for two ferromagnetic electrodes having a parallel spin orientation, and in Section B.3 for two ferromagnetic electrodes having an antiparallel spin orientation.

B.2 Parallel magnetizations

If $t^{a,\alpha} = t^{b,\beta}$, the 4×4 Dyson matrix given by equation (B.2) can be written in terms of 2×2 blocs:

$$\hat{\mathcal{D}}_{\mathrm{F}} = \begin{bmatrix} \hat{K}_{\mathrm{F}} & \hat{L}_{\mathrm{F}} \\ \hat{L}_{\mathrm{F}}^{*} & \hat{K}_{\mathrm{F}} \end{bmatrix}, \quad (B.3)$$

where $\hat{K}_{\mathrm{F}}$ and $\hat{L}_{\mathrm{F}}$ can be obtained from equation (B.2):

$$\hat{K}_{\mathrm{F}} = \begin{bmatrix} 1-K_{1,1} & K_{1,2} \\ K_{2,1} & 1-K_{2,2} \end{bmatrix}, \quad \text{and } \hat{K}_{\mathrm{AF}} = \begin{bmatrix} -L_{1,1} & L_{1,2} \\ L_{2,1} & -L_{2,2} \end{bmatrix}.$$

$$\langle\langle \mathrm{Im}\left[g_{2,1}^{\beta,\alpha}t^{\alpha,a}G_{1,1}^{a,\beta}\right]\rangle\rangle = -\frac{1}{2}\pi\rho_0^S f(\Delta_{\alpha,\beta})\left[-\frac{x_\uparrow}{1+x_\uparrow}\left(\frac{a_0}{R_{\alpha,\beta}}\right)^2 + \frac{x_\uparrow^2}{(1+x_\uparrow)^2}\frac{a_0^3}{R_{\alpha,\beta}R_{\alpha',\beta}R_{\alpha,\alpha'}}\right] \tag{B.4}$$

$$\begin{aligned}\langle\langle \mathrm{Im}\left[-g_{2,2}^{\beta,\alpha}t^{\alpha,a}G_{2,1}^{a,\beta}\right]\rangle\rangle = &-\frac{t}{(1-K_{1,1})^2(1-K_{2,2})^2}\tilde{g}_{2,2}^{\beta,\alpha}\Big\{-K_{2,1}(1-K_{1,1})(1-K_{2,2})\tilde{K}_{1,1}^{a,\beta}\\ &-\frac{1}{2}(1-K_{2,2})(1-K_{1,1})^2\tilde{K}_{2,1}^{a,\beta} - \Big[K_{2,1}\left(\tilde{L}_{1,1}(1-K_{2,2})+\tilde{L}_{2,2}(1-K_{1,1})\right)\\ &+\frac{1}{2}\tilde{L}_{2,1}(1-K_{1,1})(1-K_{2,2})\Big]\tilde{K}_{1,1}^{b,\beta} - \frac{1}{2}\tilde{L}_{2,2}(1-K_{1,1})^2\tilde{K}_{2,1}^{b,\beta}\Big\}\end{aligned} \tag{B.5}$$

$$\langle\langle \mathrm{Im}\left[g_{2,1}^{\beta,\alpha'}t^{\alpha',a'}G_{1,1}^{a',\beta}\right]\rangle\rangle = -\frac{1}{2}\pi\rho_0^S f(\Delta_{\alpha',\beta})\left[-\frac{x\uparrow}{1+x_\uparrow}\left(\frac{a_0}{R_{\alpha',\beta}}\right)^2 + \frac{x_\uparrow^2}{(1+x_\uparrow^2}\frac{a_0^3}{R_{\alpha,\beta}R_{\alpha',\beta}R_{\alpha,\alpha'}}\right] \tag{B.6}$$

$$\begin{aligned}\langle\langle \mathrm{Im}\left[-g_{2,2}^{\beta,\alpha'}t^{\alpha',a'}G_{2,1}^{a',\beta}\right] = &-\frac{t}{(1-K_{1,1})^2(1-K_{2,2})^2}\tilde{g}^{\beta,\alpha'}\Big\{\Big[-K_{2,1}\left(\tilde{L}_{1,1}(1-K_{2,2})+\tilde{L}_{2,2}(1-K_{1,1})\right)\\ &-\frac{1}{2}\tilde{L}_{2,1}(1-K_{1,1})(1-K_{2,2})\Big]\tilde{K}_{1,1}^{a,\beta} - \frac{1}{2}\tilde{L}_{2,2}(1-K_{1,1})^2\tilde{K}_{2,1}^{a,\beta}\\ &-K_{2,1}(1-K_{1,1})(1-K_{2,2})\tilde{K}_{1,1}^{a',\beta} - \frac{1}{2}(1-K_{2,2})(1-K_{1,1})^2\tilde{K}_{2,1}^{a',\beta}\Big\},\end{aligned} \tag{B.7}$$

$$\langle\langle \mathrm{Im}\left[g_{2,1}^{\beta,\alpha}t^{\alpha,a}G_{1,1}^{a,\beta}\right]\rangle\rangle = -\frac{1}{2}\pi\rho_0^S f(\Delta_{\alpha,\beta})\left[-\frac{x_\uparrow}{1+x_\uparrow}\left(\frac{a_0}{R_{\alpha,\beta}}\right)^2 + \frac{x_\uparrow x_\downarrow}{(1+x_\uparrow)(1+x_\downarrow)}\frac{a_0^3}{R_{\alpha,\beta}R_{\alpha',\beta}R_{\alpha,\alpha'}}\right] \tag{B.8}$$

$$\begin{aligned}\langle\langle \mathrm{Im}\left[-g_{2,2}^{\beta,\alpha}t^{\alpha,a}G_{2,1}^{a,\beta}\right]\rangle\rangle = &-\frac{t}{(1-K_{1,1})(1-K_{2,2})}\tilde{g}_{2,2}^{\beta,\alpha}\Big\{-K_{2,1}\tilde{K}_{1,1}^{a,\beta} - \frac{1}{2}(1-K_{1,1})\tilde{K}_{2,1}^{a,\beta} - \frac{1}{2}\tilde{L}_{2,2}\tilde{K}_{2,1}^{b,\beta}\\ &-\frac{1}{1-K_{2,2}}\left[K_{2,1}\tilde{L}_{1,1}+K_{1,2}\tilde{L}_{2,2}+\frac{1}{2}\tilde{L}_{2,1}(1-K_{1,1})\right]\tilde{K}_{1,1}^{b,\beta}\Big\}\end{aligned} \tag{B.9}$$

$$\langle\langle \mathrm{Im}\left[g_{2,1}^{\beta,\alpha'}t^{\alpha',a'}G_{1,1}^{a',\beta}\right]\rangle\rangle = -\frac{1}{2}\pi\rho_0^S f(\Delta_{\alpha',\beta})\left[-\frac{x_\downarrow}{1+x_\downarrow}\left(\frac{a_0}{R_{\alpha',\beta}}\right)^2 + \frac{x_\uparrow x_\downarrow}{(1+x_\uparrow)(1+x_\downarrow)}\frac{a_0^3}{R_{\alpha,\beta}R_{\alpha',\beta}R_{\alpha,\alpha'}}\right] \tag{B.10}$$

$$\begin{aligned}\langle\langle \mathrm{Im}\left[-g_{2,2}^{\beta,\alpha'}t^{\alpha',a'}G_{2,1}^{a',\beta}\right]\rangle\rangle = &\pi\rho_0^S\frac{t}{(1-K_{1,1})^2(1-K_{2,2})^2}\Big\{(1-K_{2,2})\left[K_{1,2}\tilde{L}_{2,2}+K_{2,1}\tilde{L}_{1,1}+\frac{1}{2}\tilde{L}_{1,2}(1-K_{2,2})\right]\tilde{K}_{1,1}^{a,\beta}\\ &+\frac{1}{2}\tilde{L}_{1,1}(1-K_{1,1})(1-K_{2,2})\tilde{K}_{2,1}^{a,\beta} + \frac{1}{2}(1-K_{1,1})(1-K_{2,2})^2\tilde{K}_{2,1}^{b,\beta} + K_{1,2}(1-K_{1,1})(1-K_{2,2})\tilde{K}_{1,1}^{b,\beta}\Big\}\cdot\end{aligned} \tag{B.11}$$

The inverse of $\hat{\mathcal{D}}_{\mathrm{F}}$ given by (B.3) takes the form

$$\hat{\mathcal{D}}_{\mathrm{F}}^{-1} = \begin{bmatrix} \hat{M}_{\mathrm{F}}^{-1} & -\hat{K}_{\mathrm{F}}^{-1}\hat{L}_{\mathrm{F}}\hat{N}_{\mathrm{F}}^{-1} \\ -\hat{K}_{\mathrm{F}}^{-1}\hat{L}_{\mathrm{F}}^{*}\hat{M}_{\mathrm{F}}^{-1} & \hat{N}_{\mathrm{F}}^{-1}\end{bmatrix},$$

with $\hat{M}_{\mathrm{F}} = \hat{K}_{\mathrm{F}} - \hat{L}_{\mathrm{F}}\hat{K}_{\mathrm{F}}^{-1}\hat{L}_{\mathrm{F}}^{*}$ and $\hat{N}_{\mathrm{F}} = \hat{K}_{\mathrm{F}} - \hat{L}_{\mathrm{F}}^{*}\hat{K}_{\mathrm{F}}^{-1}\hat{L}_{\mathrm{F}}$. The matrix in equation (B.3) can be evaluated explicitly to obtain the different terms in the Green's function (B.1):

See equation (B.4–B.7) above

where $x_\uparrow$ and $x_\downarrow$ are given by equations (7, 8). The function $f(\Delta)$ is given by $f(\Delta) = \Delta/\sqrt{\omega^2 - \Delta^2}$. The phase contribution has been factored out in the coefficients $\tilde{L}_{i,j}$. For instance, $L_{1,1} = \tilde{L}_{1,1}\exp(\mathrm{i}\varphi_{\alpha,\beta})\exp(\mathrm{i}\psi_{\alpha,\beta})$, with $\tilde{L}_{1,1} = -\pi^2 t^2\rho_\uparrow^F\rho_0^S\,(a_0/R_{\alpha,\beta})$. To obtain equation (54) we use a simplification of equations (B.4–B.7) in which equations (B.4–B.7) are transformed into a local equation. This is done by replacing $\Delta_{\alpha,\beta}$ and $\Delta_{\alpha',\beta}$ with Δ_β.

B.3 Antiparallel magnetizations

The case of an antiparallel spin orientation of the ferromagnetic electrodes can be treated in a similar manner. Once the lines and columns 3 and 4 have been interchanged, the Dyson matrix given by equation (B.2) takes the form

$$\hat{\mathcal{D}}_{\mathrm{AF}} = \begin{bmatrix} \hat{K}_{\mathrm{AF}} & \hat{L}_{\mathrm{AF}} \\ \hat{L}_{\mathrm{AF}}^{*} & \hat{L}_{\mathrm{AF}}^{*}\end{bmatrix},$$

with

$$\hat{K}_{\mathrm{AF}} = \begin{bmatrix} 1-K_{1,1} & K_{1,2} \\ K_{2,1} & 1-K_{2,2}\end{bmatrix},$$

$$\text{and } \hat{L}_{\mathrm{AF}} = \begin{bmatrix} L_{1,2} & -L_{1,1} \\ -L_{2,2} & L_{2,1}\end{bmatrix}.$$

The inverse is given by

$$\hat{\mathcal{D}}_{\mathrm{AF}}^{-1} = \begin{bmatrix} \hat{M}_{\mathrm{AF}}^{-1} & -\hat{K}_{\mathrm{AF}}^{-1}\hat{L}_{\mathrm{AF}}(\hat{M}_{\mathrm{AF}}^{*})^{-1} \\ -(\hat{K}_{\mathrm{AF}}^{*})^{-1}\hat{L}_{\mathrm{AF}}^{*}\hat{M}_{\mathrm{AF}}^{-1} & (\hat{M}_{\mathrm{AF}}^{*})^{-1}\end{bmatrix},$$

with $\hat{M}_{\mathrm{AF}} = \hat{K}_{\mathrm{AF}} - \hat{L}_{\mathrm{AF}}(\hat{K}_{\mathrm{AF}}^{*})^{-1}\hat{L}_{\mathrm{AF}}^{*}$. The different terms in the Green's function (B.1) are the following:

See equation (B.8–B.11) above.

Using a "local" approximation in which $\Delta_{\alpha,\beta}$ and $\Delta_{\alpha',\beta}$ are replaced by Δ_β leads to equation (53).

References

1. G.B. Lesovik, T. Martin, G. Blatter, `arXiv:cond-mat/0009193`.
2. M.S. Choi, C. Bruder, D. Loss, Phys. Rev. B **62**, 13569 (2000); P. Recher, E.V. Sukhorukov, D. Loss, Phys. Rev. B **63**, 165314 (2001).
3. G. Deutscher, D. Feinberg, App. Phys. Lett. **76**, 487 (2000).
4. G. Falci, D. Feinberg, F.W.J. Hekking, Europhys. Lett. **54**, 255 (2001).
5. R. Mélin, J. Phys. Cond. Matt. **13**, 6445 (2001); R. Mélin, in the *Proceedings of the XXXVIth Rencontres de Moriond*, edited by T. Martin, G. Montambaux, J. Trân Thanh Vân (EDP Sciences, 2001), p. 547.
6. R. Mélin, D. Feinberg, `cond-mat/0105329`, Eur. Phys. J. B, to appear.
7. P. Fulde, A. Ferrel, Phys. Rev. **135**, A550 (1964).
8. A. Larkin, Y. Ovchinnikov, Sov. Phys. JETP **20**, 762 (1965).
9. M.A. Clogston, Phys. Rev. Lett. **9**, 266 (1962).
10. E.A. Demler, G.B. Arnold, M.R. Beasley, Phys. Rev. B **55**, 15174 (1997).
11. A.I. Buzdin, L.N. Bulaevskii, S.V. Panyukov, JETP Lett. **35**, 178 (1982) [Zh. Eksp. Teor. Fiz. **35**, 147 (1982)]; A. Buzdin, B. Bujicic, M.Yu. Kupriyanov, Sov. Phys. JETP **74**, 124 (1992) [Zh. Eksp. Teor. Fiz. **101**, 231 (1992)].
12. V.V. Ryazanov, V.A. Oboznov, A.Yu. Rusanov, A.V. Veretennikov, A.A. Golubov, J. Aarts, Phys. Rev. Lett. **86**, 2427 (2001).
13. T. Kontos, M. Aprili, J. Lesueur, X. Grison, Phys. Rev. Lett. **86**, 304 (2001).
14. M.J.M. de Jong, C.W. Beenakker, Phys. Rev. Lett. **74**, 1657 (1995).
15. R.J. Soulen *et al.*, Science **282**, 85 (1998).
16. S.K. Upadhyay *et al.*, Phys. Rev. Lett. **81**, 3247 (1998).
17. V.T. Petrashov, V.N. Antonov, S.V. Maksimov, R. Shalkhaldarov, JETP Lett. **59**, 551 (1994).
18. M.D. Lawrence, N. Giordano, J. Phys. Cond. Matt. **39**, L563 (1996).
19. V.A. Vas'ko, V.A. Larkin, P.A. Kraus, K.R. Nikolaev, D.E. Grupp, C.A. Nordman, A.M. Goldman, Phys. Rev. Lett. **78**, 1134 (1997).
20. M. Giroud, H. Courtois, K. Hasselbach, D. Mailly, B. Pannetier, Phys. Rev. B **58**, R11872 (1998).
21. V.T. Petrashov, I.A. Sosnon, I. Cox, A. Parsons, C. Troadec, Phys. Rev. Lett. **83**, 3281 (1999).
22. A.T. Filip, B.H. Hoving, F.J. Jedema, B.J. van Wees, B. Dutta, S. Borghs, Phys. Rev. B **62**, 9996 (2000).
23. V.I. Fal'ko, C.J. Lambert, A.F. Volkov, JETP Lett. **69**, 532 (1999).
24. J.J. Jedema, B.J. van Wees, B.H. Hoving, A.T. Filip, T.M. Klapwijk, Phys. Rev. B **60**, 16549 (1999).
25. H. Imamura, S. Takahashi, S. Maekawa, Phys. Rev. B **59**, 6017 (1999).
26. I. Zütić, O.T. Valls, Phys. Rev. B **60**, 6320 (1999); I. Zütić, O.T. Valls Phys. Rev. B **61**, 1555 (2000).
27. S. Kashiwaya, Y. Tanaka, N. Yoshida, M.R. Beasley, Phys. Rev. B **60**, 3572 (1999).
28. J.-X. Zhu, B. Friedman, C.S. Ting, Phys. Rev. B **59**, 9558 (1999).
29. R. Fazio, C. Lucheroni, Europhys. Lett. **45**, 707 (1999).
30. R. Mélin, Europhys. Lett. **51**, 202 (2000).
31. J.X. Zhu, C.S. Ting, Phys. Rev. B **61**, 1456 (2000).
32. K. Halterman, O.T. Valls, `cond-mat/0107232`.
33. A.I. Buzdin, M.Yu. Kupriyanov, JETP Lett. **52**, 487 (1990); A.I. Buzdin, M.Yu. Kupriyanov, B. Vujicic, Physica C **185–189**, 2025 (1991).
34. J.S. Jiang, D. Davidović, D.H. Reich, C.L. Chien, Phys. Rev. Lett. **74**, 314 (1995).
35. C.L. Chien, J.S. Jiang, J.Q. Xiao, D. Davidović, D.H. Reich, J. Appl. Phys. **81**, 5358 (1997).
36. L.V. Mercaldo, C. Attanasio, C. Coccorese, L. Maritato, S.L. Prischepa, M. Salvato, Phys. Rev. B **53**, 14 040 (1996).
37. J.S. Jiang, D. Davidović, D.H. Reich, C.L. Chien, Phys. Rev. B **54**, 6119 (1996).
38. Th. Muhge, N.N. Garif'yanov, Yu.V. Goryunov, G.G. Khaliullin, L.R. Tagirov, K. Westerholt, I.A. Garifullin, H. Zabel, Phys. Rev. Lett. **77**, 1857 (1996); Th. Muhge, K. Westerholt, H. Zabel, N.N. Garif'yanov, Yu.V. Goryunov, I.A. Garifullin, G.G. Khaliullin, Phys. Rev. B **55**, 8945 (1997).
39. I. Baladié, A. Buzdin, N. Ryzhanova, A. Vedyayev, Phys. Rev. B **63**, 054518 (2001); A. Buzdin, A.V. Vedyayev, N. Ryzhanova, Europhys. Lett. **48**, 686 (1999).
40. S. Oh, D. Youm, M.R. Beasley, Appl. Phys. Lett. **71**, 2376 (1997).
41. L.R. Tagirov, Phys. Rev. Lett. **83**, 2058 (1999).
42. P.G. de Gennes, Phys. Lett. **23**, 10 (1966).
43. G. Deutscher, F. Meunier, Phys. Rev. Lett. **22**, 395 (1969).
44. J.J. Hauser, Phys. Rev. Lett. **23**, 374 (1969).
45. R. Mélin, J. Phys. Cond. Matt. **13**, 6445 (2001).
46. L.V. Keldysh, Sov. Phys. JETP **20**, 1018 (1965).
47. C. Caroli, R. Combescot, P. Nozières, D. Saint-James, J. Phys. C **4**, 916 (1971); *ibid.* **5**, 21 (1972).
48. J.C. Cuevas, A. Martin-Rodero, A. Levy Yeyati, Phys. Rev. B **54**, 7366 (1996).
49. A. Martin-Rodero, F.J. Garcia-Vidal, A. Levy-Yeyati, Phys. Rev. Lett. **72**, 554 (1994).
50. M. Tinkham, *Introduction to superconductivity*, 2nd edn. (McGraw-Hill, 1996).